

**STUDY ON REQUIRED FREQUENCY BAND ALLOCATIONS**  
**FOR PASSIVE SENSORS ABOVE 275 GHz**

**For EUMETSAT**

**(Contract EUM/CO/01/935/RW)**

Intentionally left blank

**This study was performed under EUMETSAT contract**

**EUM/CO/01/935/RW by :**

Daniel BRETON  
4, rue dels Pibouls  
LACROIX-FALGARDE  
F-31120

-----  
Tel : (33)(0)5 61 76 35 57  
Fax : (33)(0)5 61 76 41 22  
e-mail : [Daniel.Breton@wanadoo.fr](mailto:Daniel.Breton@wanadoo.fr)  
-----

intentionally left blank

## Document Change Record

<i>Issue / Revision</i>	<i>Date</i>	<i>DCN. No</i>	<i>Changed Pages / Paragraphs</i>
Version 1	29/01/02		

Intentionally left blank

**STUDY ON REQUIRED FREQUENCY BAND ALLOCATIONS**  
**FOR PASSIVE SENSORS ABOVE 275 GHz**

(Contract EUM/CO/01/935/RW)

**TABLE OF CONTENTS**

1.0 : <u>INTRODUCTION</u>	11
2.0 : <u>PREFERRED ALLOCATIONS</u>	13
2.1 : <u>Characterization of the atmosphere in various climate conditions</u>	13
2.2 : <u>Identification of candidate frequency bands for passive sensing</u>	15
<b>2.2.1 : Vertical atmospheric temperature and humidity sounding</b>	15
2.2.1.1 : <i>General remarks</i>	15
2.2.1.2 : <i>Vertical temperature sounding</i>	17
<b>2.2.2 : Identification of candidate frequency bands for limb sounding</b>	17
3.0 : <u>MAIN CHARACTERISTICS OF PASSIVE SENSORS</u>	19
3.1 : <u>General</u>	19
3.2 : <u>Review of existing and planned sensors in the spectral region of interest</u>	19
3.3 : <u>Elaboration of representative study scenarios</u>	20
4.0 : <u>POTENTIAL INTERFERENCE TO THE LIMB SOUNDERS</u>	22
4.1 : <u>Budget of potential interference from Active Terrestrial Service</u>	22
<b>4.1.1 : Geometry of interference</b>	22
<b>4.1.2 : Maximum acceptable interfering power density</b>	23
4.1.2.1 : <i>Atmosphere model</i>	23
4.1.2.2 : <i>Atmospheric absorption depending on elevation angle of the interfering path</i>	24
4.1.2.3 : <i>Path loss depending on elevation angle of the interfering path</i>	25
4.1.2.4 : <i>Effective area of the sensor antenna in direction of the earth's surface</i>	26
4.1.2.5 : <i>Maximum acceptable EIRP density in direction of the sensor</i>	27
<b>4.1.3 : Results of the simulation</b>	29
4.1.3.1 : <i>General remarks</i>	29
4.1.3.2 : <i>Discussion of the results</i>	29
4.1.3.3 : <i>Preliminary conclusion on co-frequency sharing with active terrestrial service</i>	32
4.2 : <u>Budget of potential interference from the Inter-Satellite Service</u>	33
<b>4.2.1 : Geometry of interference</b>	33
<b>4.2.2 : Maximum acceptable power flux density in the environment of the sensor</b>	34
<b>4.2.3 : Provisional sharing criteria</b>	35

5.0 : <u>POTENTIAL INTERFERENCE TO THE NADIR SOUNDERS</u>	37
5.1 : <u>Budget of potential interference to nadir sounders in LEO from Active Terrestrial Service</u>	37
5.1.1 : <b>Geometry of interference</b>	37
5.1.2 : <b>Maximum acceptable interfering power density</b>	37
5.1.2.1 : <i>Atmosphere model and frequencies adopted for the simulation</i>	37
5.1.2.2 : <i>Path loss depending on the elevation angle of the interfering path</i>	38
5.1.2.3 : <i>Effective area of the sensor's antenna in direction of the earth's surface</i>	39
5.1.2.4 : <i>Maximum acceptable EIRP density in direction of the sensor</i>	39
5.1.3 : <b>Results of the analysis</b>	39
5.2 : <u>Budget of potential interference to nadir sounders in GEO from active terrestrial service</u>	43
5.2.1 : <b>Geometry of interference</b>	43
5.2.2 : <b>Maximum acceptable interfering power density</b>	44
5.2.3 : <b>Results of the analysis</b>	48
5.3 : <u>Budget of potential interference from the Inter-Satellite Service</u>	49
5.3.1 : <b>Geometry of interference</b>	49
5.3.2 : <b>Maximum acceptable single-entry pfd in the sensor's environment</b>	50
5.3.3 : <b>Preliminary conclusion</b>	51
6.0 : <u>GENERAL SUMMARY</u>	51

## FIGURES AND TABLES

### **Section 2 : Passive sensor preferred allocations in the 275-1000 GHz frequency band**

<u>Figure 2.1</u> : Vertical opacity of the atmosphere for various climate conditions	13
<u>Table 2.1</u> : Water vapour surface density and total columnar content	14
<u>Figure 2.2</u> : Linear absorption at ground level, from recommendation ITU-R P.676	14
<u>Table 2.2</u> : Frequency allocations proposed	16
<u>Figure 2.3</u> : Frequency bands required for passive sensors in the 275-1000 GHz region	18

### **Section 3 : Main characteristics of passive sensors**

<u>Table 3.1</u> : Main characteristics of existing and planned passive sensors	20
<u>Table 3.2</u> : Technical parameters of study scenarios	21

### **Section 4 : Potential interference to the limb sounders**

<u>Figure 4.1.1</u> : Geometry of potential interference from active terrestrial service	22
<u>Figure 4.1.2</u> : Iso-gain lines of the sensor's antenna, projected on the earth's surface	23
<u>Figure 4.1.3</u> : Vertical opacity due to H <sub>2</sub> O+O <sub>2</sub> lines and wet+dry continuum	24
<u>Figure 4.1.4</u> : Average lengthening factor for the lowest 5 km-thick atmospheric layer	25
<u>Figure 4.1.5</u> : Total propagation losses between the earth's surface and the sensor	26



<u>Figure 4.1.6</u> : Sensor antenna effective area in direction of the earth's surface	27
<u>Table 4.1.1</u> : Maximum EIRP density (dBW/MHz) at low elevation angles (num.)	28
<u>Figure 4.1.7</u> : Maximum EIRP density around 275 GHz	29
<u>Figure 4.1.8</u> : Maximum EIRP density around 670 GHz	30
<u>Figure 4.1.9</u> : Maximum EIRP density around 860 GHz	30
<u>Table 4.1.2</u> : Foot-print of the passive sensor antenna at grazing angle	31
<u>Table 4.1.3</u> : Proposed Global EIRP density limits	32
<u>Table 4.1.4</u> : Single-entry EIRP density limits (num.) applicable to ground transmitters	32
<u>Figure 4.2.1</u> : Geometry of potential interference from the Inter-Satellites Service	33
<u>Table 4.2.1</u> : Relative contribution of ISS links in sensor's antenna main and first secondary lobes	34
<u>Table 4.2.2</u> : Maximum acceptable contribution of the ISS to the interference threshold	35
<u>Figure 4.2.2</u> : Maximum single-entry PFD at the level of the sensor	35
<u>Table 4.2.3</u> : Maximum PFD (num.) depending on $\Delta T_e$ and frequency	36

## **Section 5 : Potential interference to the nadir sounders**

<u>Figure 5.1.1</u> : Geometry of potential interference from terrestrial active service	37
<u>Table 5.1.1</u> : Frequency bands and minimum vertical absorption	38
<u>Figure 5.1.2</u> : Total propagation losses between the earth's surface and the sensor	38
<u>Figure 5.1.3</u> : Sensor antenna effective area in direction of the earth's surface	39
<u>Figure 5.1.4</u> : Maximum EIRP density for required $\Delta T_e = 0.5$ K	40
<u>Table 5.1.2</u> : Summary results of the analysis for nadir sounders in LEO	40
<u>Figure 5.1.5</u> : Maximum acceptable EIRP density for required $\Delta T_e = 0.1$ K	41
<u>Figure 5.1.6</u> : Maximum acceptable EIRP density for required $\Delta T_e = 0.02$ K	41
<u>Table 5.1.3</u> : Maximum EIRP density (dBW/MHz) around zenith (num.)	42
<u>Table 5.2.1</u> : Specific features of climatic zones as seen from nadir sonder in GSO	43
<u>Figure 5.2.1</u> : Geometry of potential interference from active terrestrial service	44
<u>Figure 5.2.2</u> : Total propagation loss between the earth's surface and the sensor	45
<u>Figure 5.2.3</u> : Sensor antenna effective area in direction of the earth's surface	45
<u>Figure 5.2.4</u> : Maximum EIRP density for required $\Delta T_e = 0.5$ K	46
<u>Figure 5.2.5</u> : Maximum EIRP density for required $\Delta T_e = 0.1$ K	46
<u>Table 5.2.2</u> : Maximum EIRP density (dBW/MHz) at low elevation angle	47
<u>Figure 5.2.6</u> : Maximum EIRP density for required $\Delta T_e = 0.02$ K	48
<u>Table 5.2.3</u> : Summary results of the analysis for nadir sounders in GSO and in LEO	48
<u>Figure 5.3.1</u> : Geometry of potential interference from the ISS	49
<u>Table 5.3.2</u> : Single-entry pfd limit at the level of nadir sounders in LEO and in GSO	50

## **Section 6 : General summary**

<u>Table 6.1</u> : Limb sounders, single-entry EIRP limits applicable to ground transmitters	51
<u>Figure 6.1</u> : Limb sounders, Maximum single-entry spectral pfd at the level of sensor	51
<u>Table 6.2</u> : Nadir sounders in GSO and LEO, Max.EIRP density from terrest..services	52
<u>Figure 6.2</u> : Nadir sounders in GSO and LEO, single-entry spectral pfd from the ISS	52

## **LIST OF ACRONYMS**

ATM :	Atmospheric Transmission at Microwave
EESS :	Earth Exploration Satellite Service
EIRP :	Equivalent Isotropic Radiated Power
GSO :	GeoStationary Orbit
ISS :	Inter-Satellite Service
ITU :	International Telecommunication Union
LEO :	Low Earth Orbit
MLS :	Microwave Limb Sounding
PDRR :	Preliminary Draft Revised Recommendation
PFD :	Power Flux Density
SFCG :	Space Frequency Coordination Group
SSO :	Sun Synchronous Orbit
WRC :	World Radio Conference

**STUDY ON REQUIRED FREQUENCY BAND ALLOCATIONS**  
**FOR PASSIVE SENSORS ABOVE 275 GHz**

(Contract EUM/CO/01/935/RW)

1.0 : INTRODUCTION

Passive sensors can suffer interference from "active services" allocated in the same frequency band or in adjacent bands.

In the perspective of the WRC-2003 (World Radio Conference), frequency allocations to the microwave passive sensors are being reviewed and several studies are being pursued or undertaken to determine the levels of protection against interference which are necessary to ensure satisfactory operations of these sensors in the frequency bands allocated.

The objectives depend on the frequency band considered:

- ✘ ***In the band 1 to 71 GHz*** , studies are going on since several years to improve as far as feasible the status of passive sensors allocations. The situation is not flexible because many active services are already deployed in this spectral region, within or close to the bands allocated to the passive sensors ; it is often necessary to come to a compromise, for instance accept a data availability lower than required. A number of significant results were obtained at WRC-1997 and WRC-2000, but some questions are still to be addressed, in particular the protection of passive sensors from unwanted emissions in frequency bands below 60 GHz, which is the subject of Study II of this contract;
- ✘ ***In the band 71 to 275 GHz*** , a spectral region which is still largely unused, very good results were obtained at WRC-2000. They have yet to be confirmed by appropriate sharing studies, as soon as objectives and technical characteristics of active services will be known ;
- ✘ ***In the band 275 to 1000 GHz*** , there is for the time being no allocation. To prepare the basis for a completely new table of allocations, including estimate of sensor's performance and protection levels, is the subject of Study I of this contract. Because the scientific experience in the utilization of this spectral region is still uncomplete and scientific requirements are not firmly established, it must be emphasized that at this stage, such a study can only be a first approach. Conclusions which are proposed are preliminary and should be considered as a basis for discussion.

Concerning the frequency range 71 to 1000 GHz, it is important to emphasize that :

- ✘ There are to day very few « active » applications, if any, already deployed in this part of the spectrum, and the situation is still very flexible. It is therefore possible and highly desirable to avoid compromises which can have a detrimental effect to the operations of passive sensors ;

- ⌘ The levels of protection which are necessary to ensure adequate operations of passive sensors are derived from estimates of their performances which are likely to be required in a t.b.d. future from a purely scientific viewpoint. Technological concerns should not be considered and should not be a limit at this stage ;
- ⌘ After an agreement is reached on a protection level in a particular frequency band (for instance at WRC-2003), it is expectable that interference will progressively increase up to the agreed levels while active services are being deployed, thus precluding further improvements of the passive sensor in that band.

It is clear therefore that the estimates of passive sensor's requirements and protection criteria which are made to day, commit the future of this sensing technique and should not be limited to the to day's needs.

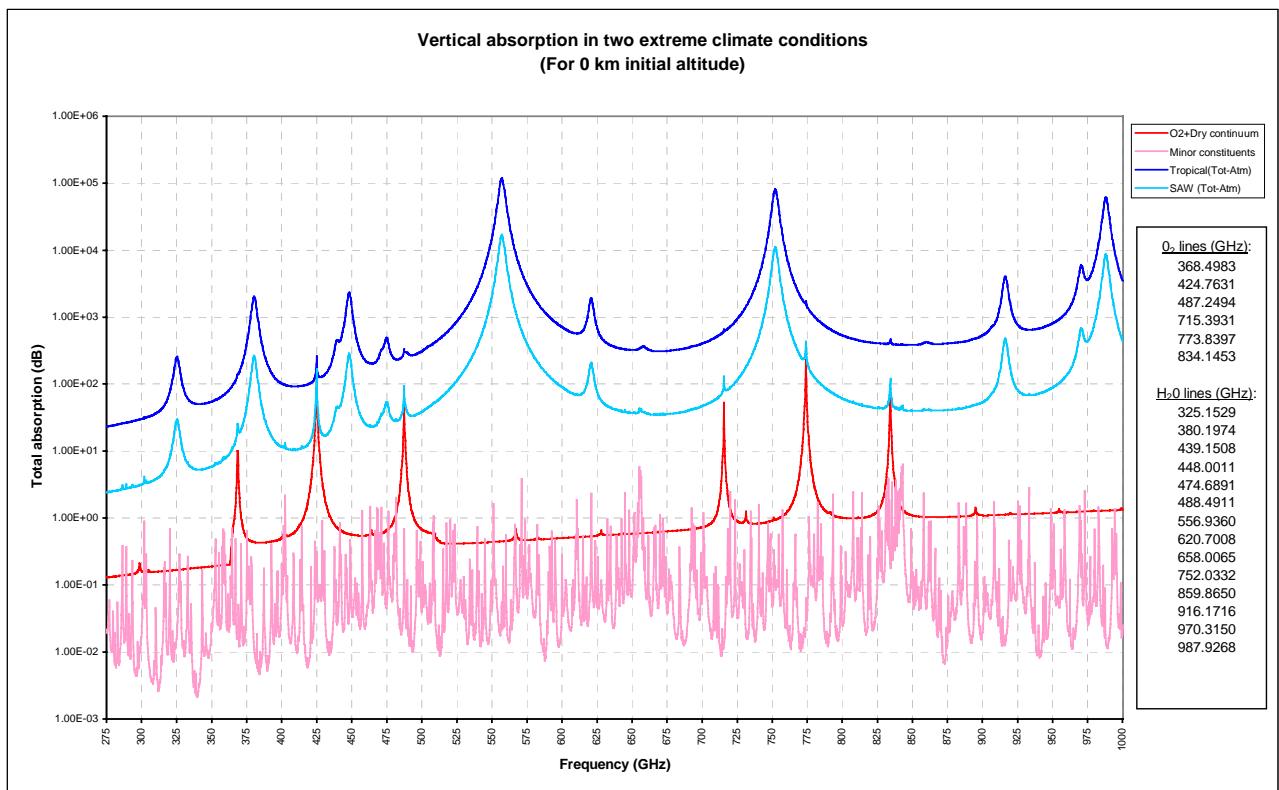
**For that reason the sensor's performances which are adopted in this study include figures which may be significantly better than those proposed in the currently existing documents. Considering the speculative aspect of this study and the great difficulties which were in the past, and are still to day, encountered by the scientific community in its attempts to secure/improve frequency allocations for passive sensors, it is strongly recommended to adopt the most ambitious, yet scientifically justified, requirements.**

## 2-0 : PASSIVE SENSOR PREFERRED ALLOCATIONS IN THE 275-1000 GHZ FREQUENCY BAND

### 2.1 Characterization of the atmosphere in various climate conditions :

The atmosphere model ATM (Atmospheric Transmission at Microwaves, J.R.Pardo, J.Cernicharo, E.Serabyn) is used for this study. The *figure 2.1* shows the vertical opacity of the atmosphere due to absorption by water vapour (resonances and continuum), oxygen (resonances and dry continuum) and minor constituents for 0 km initial altitude. For all climate conditions, the absorption by water vapour dominates largely the effects of other components, even in presence of oxygen resonances, and varies significantly depending on the local climate and seasonal conditions. Because the atmospheric water vapour is essentially concentrated in the troposphere, this suggests that sounding at these frequencies may not go far below the tropopause (around 10 km, depending on local climate/weather conditions).

Figure 2.1 : Vertical opacity of the atmosphere for various climate conditions



The recommendation ITU-R P.836 (International Telecommunication Union) provides worldwide maps of the atmospheric water vapour content at ground level. These maps are yearly averages, calculated on the basis of 10 years radiosonde data for 323 sites all over the world, covering more or less all climate regions. The *table 2.1* compares the values of water vapour density and total columnar content at ground level, as given by the ATM model and the ITU recommendation, and shows a fair correspondence.

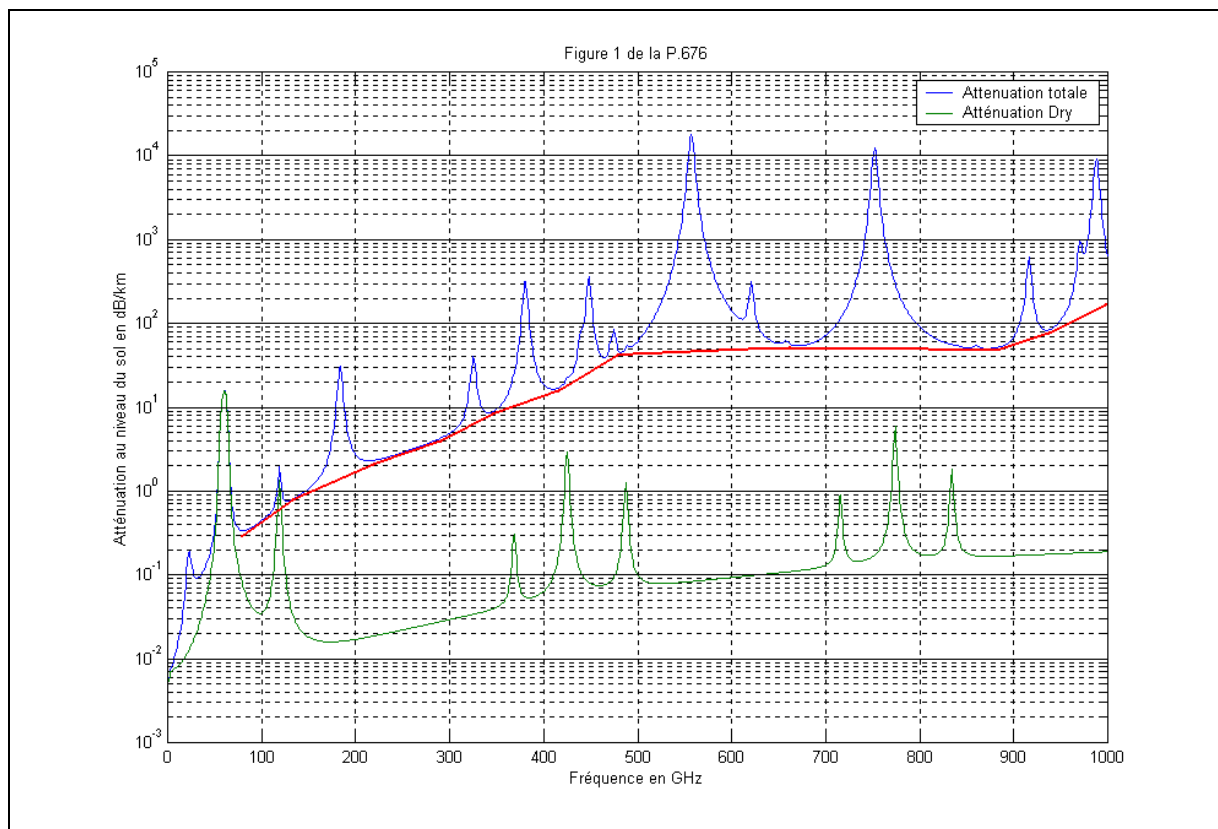
The statistical indication given in the recommendation concerning the total columnar content (exceeded for 10%, or not exceeded for 90%, of the average year) is interesting and shows that water vapour as an essential, but unreliable shielding parameter against interference generated from the earth's surface must be considered with great care.

Table 2.1 : Water vapour surface density and total columnar content

Climate/season	Rec.ITU-R P.836		ATM model	
	Surf.dens.(g/m3)	Tot.column (kg/m2)	Surf.dens.(g/m3)	Tot.column (kg/m2)
<b>Tropical</b>	20 to 25	< 50 (90% of time)	18	41
<b>Mid-lat.summer</b>	10 to 15	< 30.(90% of time)	13.5	29.5
<b>Mid-lat.winter</b>	5 to 10	< 30 (90% of time)	3.5	8.6
<b>Sub-arct.summer</b>	5 to10	< 22 (90% of time)	8.7	21
<b>Sub-arc.winter</b>	2 to 5	< 22 (90% of time)	1.3	4.2

The linear absorption at ground level is also an essential parameter which must be taken into consideration for the implementation of active terrestrial services. The linear absorptions due to the dry components and due to the dry + humid components are shown on the *figure 2.2*. The water vapour is largely the dominant parameter. The magnitude of linear absorption at ground level will be used in the study to evaluate the density of potential interfering terrestrial services which may be within the sensor's field of view. Above 275 GHz, the linear absorption is extremely high due to the vicinity of multiple powerful resonances, ranging from approximately 35 dB/km in the lowest part of the frequency band considered, up to more than  $10^4$  dB/km in the most powerful H<sub>2</sub>O absorption lines ; this might be attractive for the deployment in very large quantities of very short range terrestrial services such as links of the Fixed Service or collision avoidance radars on cars.

Figure 2.2 : Linear absorption at ground level, from recommendation ITU-R P.676



## 2.2 Identification of candidate frequency bands for passive sensing :

The *table 2.2* contains the list of candidate frequency bands for microwave passive sensing from 275 GHz to 1000 GHz. This table is based on the Preliminary Draft Revised Recommendation (PDRR) ITU-R SA.515-3, which is not yet finalized. Proposed frequencies and associated requirements resulting from the recent review of this PDRR the SFCG-21 (Space Frequency Coordination Group) are underlined.

A number of new inputs were also introduced :

- ✘ The frequencies which are, or will be used by existing and planned projects, as far as they are not already proposed in the preliminary draft revised recommendation ;
- ✘ Recent inputs and comments from the scientific community. They provisionally include also requirements for ground based and airborne measurements, which might be more appropriately merged with Radio Astronomy requirements (to be verified).

The *figure 2.3* shows the position of the frequency bands originally proposed in the PDRR 515 in the atmosphere absorption spectrum between 275 and 1000 GHz. The significance of this figure is clear when considering the frequency bands proposed for vertical sounding around O<sub>2</sub> and H<sub>2</sub>O lines.

### **2.2.1 : Vertical atmospheric temperature and humidity sounding :**

#### *2.2.1.1 : General remarks*

As a preliminary recommendation, it is important to stress that, where the selection of a frequency band is proposed to perform vertical temperature or humidity sounding, it is important to retain the two wings of the absorption line, because the utilization of symmetric channels on both sides of the peak at similar absorption levels is equivalent to doubling the bandwidth, thus improving the signal to noise ratio, without degrading the vertical resolution of the instrument as would be the case, should a unique, wider channel on one single side of the peak be used.

After several up and down fluctuations, the « required  $\Delta T_e$  » for nadir sounding in the preliminary draft revised recommendation are now ranging from 0.2 to 0.5 K. Considering that they are supposed to express the future requirements within a 10 to 15 years time frame, these figures seem surprisingly down on previous proposals. The rationale which led to the adoption of such figures is unclear : In the opinion of the author, they should be based on purely scientific considerations projected several years ahead, ignore any to-day technological limitation, and should be carefully checked before being definitively adopted.

Window channels which must be associated to the measurements performed around the absorption lines are not clearly identified.

They should be selected close enough to the H<sub>2</sub>O and O<sub>2</sub> resonances selected, but in bands where the vertical absorption is the lowest. Considering the magnitude of the vertical absorption in the spectral region of interest, it might be more appropriate to select a window below 275 GHz.

However, window channels could be proposed in bands identified for limb measurement of minor species, provided that these bands are close enough to the absorption line considered, and placed in a « valley » of the H<sub>2</sub>O absorption spectrum.

Table 2.2 : Frequency allocations proposed

Proposed allocation (GHz)	Total BW required (GHz)	$\Delta T_e$ required (K)	Data availability (%)	Geophysical parameter	Scanning conf. (Nadir, Limb)	Comments, Existing and planned sensors
<u>275-277</u> (1)	<u>2</u>	<u>0.005</u>	<u>99</u>	Minor	L	Ground based measurements
<u>277-282</u> (2)	<u>5</u>		<u>99</u>	Minor	L	Ground based measurements
<u>294-306</u> (1)	<u>12</u>	<u>0.2/0.005</u> (3)	<u>99.99/99</u> (3)	Minor	N, L	MASTER
<u>316-334</u> (1)	<u>18</u>	<u>0.3/0.005</u> (3)	<u>99.99/99</u> (3)	H <sub>2</sub> O pro, Min.	N, L	MASTER
<u>335-342</u> (2)	<u>7</u>		<u>99.99/99</u> (3)	Min. window	N, L	Future
<u>342-349</u> (1)	<u>7</u>	<u>0.3/0.005</u> (3)	<u>99.99/99</u> (3)	Minor	N,L	MASTER
<u>363-365</u> (1)	<u>2</u>	<u>0.005</u>	<u>99</u>		L	
<u>371-389</u> (1)	<u>18</u>	<u>0.3</u>	<u>99.99</u>	H <sub>2</sub> O prof.	N	GOMAS
<u>416-434</u> (1)	<u>18</u>	<u>0.4</u>	<u>99.99</u>	O <sub>2</sub> prof.	N	GOMAS
<u>442-444</u> (1)	<u>2</u>	<u>0.005</u>	<u>99</u>	Minor	L	
<u>459-466</u> (2)	<u>7</u>		<u>99.99</u>	Ice clouds	N	CLOUDS
<u>486-496</u> (2)	<u>10</u>		<u>99</u>	H <sub>2</sub> O	L	ODIN
<u>496-506</u> (1)	<u>10</u>	<u>0.5/0.005</u> (3)	<u>99.99/99</u> (3)	Min. window	N,L	ODIN, SOPRANO, MASTER
<u>541-546</u> (2)	<u>5</u>			Minor	L	ODIN
<u>546-568</u> (1)	<u>12</u>	<u>0.5/0.005</u> (3)	<u>99.99/99</u> (3)	H <sub>2</sub> O	N, L	ODIN
<u>568-584</u> (2)	<u>16</u>		<u>99</u>	Meso.H <sub>2</sub> O	L	ODIN
<u>606-608</u> (2)	<u>2</u>			Minor		Airborne measurements
<u>612-614</u> (2)	<u>2</u>			Minor		Airborne measurements
<u>619-622</u> (2)	<u>2</u>			Minor		Airborne measurements
<u>624-629</u> (1)	<u>5</u>	<u>0.005</u>	<u>99</u>	Minor	L	MLS, SMILES, SOPRANO, MASTER
<u>634-654</u> (1)	<u>20</u>	<u>0.5/0.005</u> (3)	<u>99.99/99</u> (3)	Min. window	N,L	MLS, SMILES, SOPRANO
<u>659-661</u> (1)	<u>2</u>	<u>0.005</u>	<u>99</u>	Minor	L	MLS (AURA)
<u>676-684</u> (2)	<u>8</u>		<u>99.99</u>	Ice clouds	N	CLOUDS
<u>684-692</u> (1)	<u>8</u>	<u>0.005</u>	<u>99</u>	Ice clouds	N,L	CLOUDS
<u>730-732</u> (1)	<u>2</u>	<u>0.005</u>	<u>99</u>	Minor	L	SOPRANO
<u>743-761</u> (2)	<u>18</u>		<u>99.99</u>	H <sub>2</sub> O prof.	N	
<u>825-843</u> (2)	<u>18</u>		<u>99.99</u>	O <sub>2</sub> prof.	N	
<u>851-853</u> (1)	<u>2</u>	<u>0.005</u>	<u>99</u>	Min. window	L	SOPRANO
<u>868-881</u> (2)	<u>13</u>		<u>99.99</u>	Ice clouds	N	CLOUDS
<u>951-956</u> (1)	<u>5</u>	<u>0.005</u>	<u>99</u>	Minor	L	SOPRANO

(1) Preliminary draft revised ITU-R SA.515-3

(2) Required by existing and planned instruments but not listed in the original recommendation, or recent inputs from the scientific community.

(3) Second number for microwave limb sounding applications



There are a number of powerful H<sub>2</sub>O lines ; several are listed in the preliminary draft revised recommendation. Three comments can be made :

- ✘ **Allocation around 325.15 GHz** seems of secondary interest as compared to the allocation around 380.2 which is more powerful.  
For both, a window channel around 345 GHz, in a band already proposed in the PDRR 515, should be appropriate ;
- ✘ **Allocation around 557 GHz** is wrongly declared as an O<sub>2</sub> line. This is in fact the strongest H<sub>2</sub>O line in the frequency band considered. The associated window channel could be selected around 500 GHz or around 640 GHz, in bands already proposed in the PDRR 515 ;
- ✘ **There is no allocation proposed above 575 GHz.** If scientifically justified, the strong H<sub>2</sub>O line at 752 GHz could be included, with a total bandwidth of 18 GHz (743-761 GHz). A window channel around 690 GHz, in a band already proposed in the PDRR 515, should be adequate.

#### *2.2.1.2 : Vertical temperature sounding*

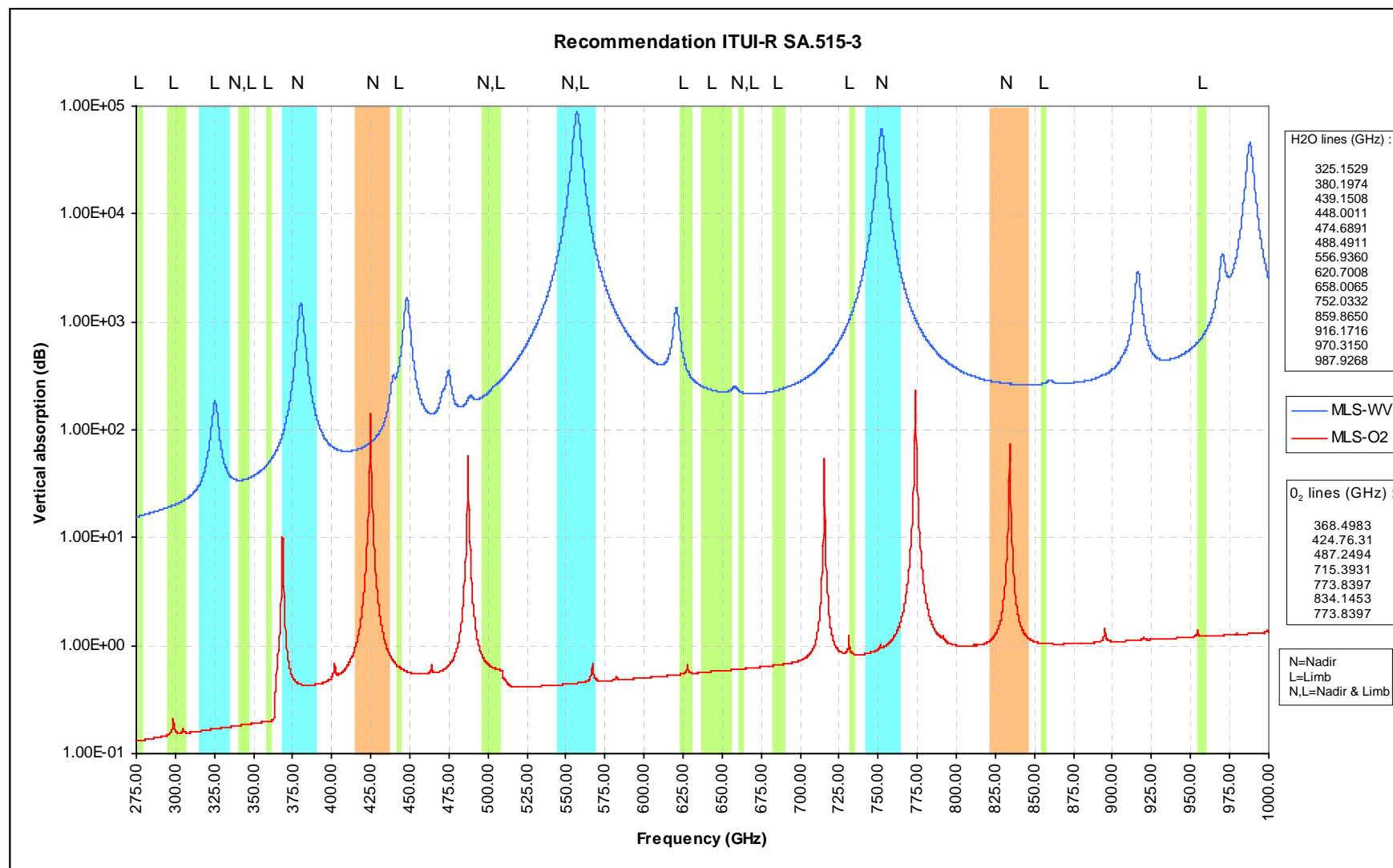
The O<sub>2</sub> lines hardly emerge from the H<sub>2</sub>O absorption spectrum, even in dry climate conditions (Sub-arctic winter). This suggests that they can be used for vertical soundings in the stratosphere and in the upper troposphere, where the H<sub>2</sub>O concentration is so low that it can be considered as a minor constituent.

- ✘ **Only one allocation is proposed in the recommendation around the O<sub>2</sub> line at 424.8 GHz** (416-434 GHz). A window channel around 500 GHz, in the closest « minimum » of the H<sub>2</sub>O absorption spectrum seems appropriate, in a frequency band already proposed in the PDRR 515 ;
- ✘ **A second allocation is suggested around the O<sub>2</sub> line at 834.15 GHz**, in a « valley » of the H<sub>2</sub>O absorption spectrum, with a similar bandwidth (825-843 GHz). A window channel in the frequency band 851-853 GHz (already proposed in the PDRR 515) seems adequate.

#### **2.2.2 Identification of candidate frequency bands for limb sounding of minor constituents :**

The absorption spectrum of minor constituents in the spectral region of interest is so dense that it is not easy , for a non specialist, to criticize the allocations proposed in the PDRR 515. Consequently the only contribution to the table 2.2 in relation to the measurement of minor constituents is the introduction of frequency bands that are required by existing and planned projects, and recent inputs from the scientific community. It is anticipated that further review of the proposed allocations by the scientific community will be necessary before final adoption in order to eliminate possibly redundant requirements.

Figure 2.3 : Frequency bands required for passive sensors in the 275-1000 GHz region



### 3.0 : MAIN CHARACTERISTICS OF PASSIVE SENSORS

#### 3.1 General

Microwave passive sensors are essential to study the atmosphere. Two types of passive sensors are used :

- ✧ **Vertical sounders** observe the atmosphere in the nadir direction. They are designed essentially to perform measurements around O<sub>2</sub> and H<sub>2</sub>O absorption lines, and are used to obtain vertical profiles of the atmosphere temperature and humidity content, which are essential parameters in meteorology to initialize the numerical weather prediction models. The utilization of the sub-mm spectrum for vertical sounding is particularly attractive for missions in geostationary orbit because it enables a good horizontal resolution while maintaining a reasonable antenna size.
- ✧ **Limb sounders** observe the atmosphere tangentially to study minor atmospheric constituents in regions where the intense photo chemistry activities may have a heavy impact on the earth's climate. The most important feature of tangential limb emission measurements is that this configuration enables the longest possible path in the absorbing medium, which maximizes signals from low-concentration (but radiatively and chemically important) atmospheric trace species, and render possible sounding of high altitude, low pressure atmospheric layers.

#### 3.2 : Review of existing and planned passive sensors in the spectral region of interest :

There is not much experience in this spectral region. Existing and planned instruments are not very many. The *table 3.1* summarizes the main relevant characteristics of a few existing and planned instruments, and compares the frequency bands that are required to the allocations proposed in the recommendation.

There is to day one sensor in operational phase (ODIN, launched in february 2001), MLS on « EOS Chem » planned in december 2002, JEM/SMILES on the international space station planned for the end of 2005 and a few other passive sensors at various definition or development stages.

**CLOUDS :** Preliminary studies ; Sun-synchronous orbit, one conically scanned (around nadir) microwave sensor working in the sub-mm region :

*CIWSIR* ( Cloud Ice and Water-vapour Sub-mm Imaging Radiometer) is a conically scanned (around nadir) sensor, with 8 channels between 150 and 875 GHz.

**GOMAS :** Preliminary studies ; Geostationary orbit, one nadir-looking microwave sensor with channels between 57 and 425 GHz.

**ODIN :** Launched in February 2001 ;

**MASTER :** Phase-A, breadboarding ; Sun-synchronous orbit 820 km.

**AURA (EOS Chem) :** Planned for December 2002. Sun-synchronous orbit 700 km altitude. One microwave sensor MLS (Microwave Limb Sounder) with channels between 118 GHz and 2.5 THz.

**JEM/SMILES :** Planned for the end of 2005 on the International Space Station. Low earth, low inclination orbit, 400 km altitude.

Table 3.1 : Main characteristics of existing and planned passive sensors

Rec.SA.515-3 (GHz)	SPECIES	ODIN	CLOUDS	GOMAS	MASTER	AURA	SMILES
		FREQUENCY BANDS SELECTED (GHz)					
294.0-306.0	O <sub>3</sub> ,N <sub>2</sub> O...	-----	-----	-----	294.0-305.5	-----	-----
316.0-334.0	H <sub>2</sub> O,O <sub>3</sub>	-----	-----	-----	316.5-325.5	-----	-----
342.0-349.0	CO,HNO <sub>3</sub> O <sub>3</sub>	-----	-----	-----	342.2-348.8	-----	-----
371.0-389.0	WV profile	-----	-----	379.0-381.0	-----	-----	-----
416.0-434.0	T° profile	-----	-----	424.5-425.5	-----	-----	-----
-----	Ice clouds	-----	459.6-465.6	-----	-----	-----	-----
496.0-506.0	O <sub>3</sub> - Minor	486.1-503.9	-----	-----	497.0-506.0	-----	-----
-----	HNO <sub>3</sub> -O <sub>3</sub>	541.0-546.0	-----	-----	-----	-----	-----
546.0-568.0	WV profile	546.0-568.0	-----	-----	-----	-----	-----
-----	Mesos.H2O	568.0-584.0	-----	-----	-----	-----	-----
624.0-629.0	Minor	-----	-----	-----	624-624.5	624.6-626.6	624.3-626.4
634.0-654.0	Minor+WV	-----	-----	-----	-----	635.7-653.5	649.1-650.4
659.0-661.0	BrO	-----	-----	-----	-----	660.3-660.6	-----
-----	Ice clouds	-----	676.9-688.9	-----	-----	-----	-----
-----	Ice clouds	-----	868.4-880.4	-----	-----	-----	-----
Main relevant parameters		TECHNICAL CHARACTERISTICS					
Orbit type/altitude (km) :			SSO/800	GSO/35900	SSO/800	SSO/700	LEO/400
Orbit inclination (°) :			98	0	98	98	52
Scanning mode :			Conical 45°	Nadir	Limb	Limb	Limb
NEAT (K) :			1.0	0.5	0.5	0.1	0.7
Antenna IFOV El x Az (°) :			0.35	0.016	0.2	0.028x0.056	0.083x0.174

### 3.3 : Elaboration of representative study scenarios

A limited number of scenarios are defined for further consideration. They include the set of minimum parameters (geometry of observation, instrument characteristics and performances) which are necessary to evaluate the susceptibility to interference and to derive protection criteria. It is assumed that potential interferers are the Inter-satellites Services and any Active Terrestrial Service, including the Fixed Service.

Only potential interference resulting from co-frequency sharing with active services will be considered.

Three scenarios are defined for detailed study. For each one, the frequency is a variable parameter. To evaluate the impact of the required performances on the protection and sharing criteria, the required radiometric resolution ( $\Delta T_e$ ) is also a variable parameter :

- ✘ One scenario for limb sounding from LEO (Low Earth Orbit) ;
- ✘ One scenario for nadir sounding from LEO ;
- ✘ One scenario for nadir sounding from GSO (GeoStationary Orbit).

The technical characteristics are given in the *table 3.2*. No assumptions are made on the receiver characteristics and on the integration time. Only the  $\Delta T_e$  which results from these parameters is considered. As a consequence, the radiometric threshold and the interference threshold are referred to the unit bandwidth (1 MHz) and are power densities which can easily be converted when real bandwidths are considered.

It is expected that these working hypothesis will be progressively refined and that study updating will become necessary in a t.b.d. future.

Table 3.2 : Technical parameters of study scenarios

Parameters	Limb Sounding	Nadir Sounding	
<b>Orbit height (km) :</b>	700	700	35900
<b>Scanning (1) :</b>	Tangential 0 km	+/- 51.3° (2)	+/- 8.2°
<b>Antenna model :</b>	Rec.ITU-R F.699-4	Rec.ITU-R F.699-4	Rec.ITU-R F.699-4
<b>Total half-power BW (°) :</b>	0.054	0.4	0.04
<b>Total main lobe BW (°) :</b>	0.15	1.2	0.12
<b>Limit 40 dBi (°) :</b>	1.0	-----	1.0
<b>Limit 30 dBi (°) :</b>	2.4	-----	2.4
<b>Limit 20 dBi (°) :</b>	6	-----	6
<b>Limit 10 dBi (°) :</b>	15.2	-----	15.2
<b>Isotropic gain (dBi) :</b>	70	53	72.5
<b>Ant.diameter at 275 GHz (cm) :</b>	142	20	142
<b>Cold space cal.ant. (dBi) (3) :</b>	70	35	35
<b>Horizontal resolution (km) :</b>	N/A	5	25
<b>Radiometric resolution (K) :</b>	0.1/0.01/0.001	0.5/0.1/0.02	0.5/0.1/0.02
<b>Radiometric threshold (dBW/MHz) :</b>	-179/-189/-199	-172/-179/-186	-172/-179/-186
<b>Interference threshold (dBW/MHz) :</b>	-186/-196/-206	-179/-186/-193	-179/-186/-193

- (1) The scanning angle of the nadir sounders is limited by the maximum incidence angle 60° (LEO) and 70° (GSO) at the earth's surface ; Note that sounders in GSO must scan in two orthogonal directions N/S and E/W.
- (2) A cross-track scanner, more vulnerable to interference than the conical scanner proposed in « CLOUDS », is considered in the analysis.
- (3) For limb sounders, cold-space calibration is implemented during the normal vertical scanning of the sensor. A specific, lower gain, antenna is assumed to be required for nadir sounders.

Various yet unidentified « active services » can potentially interfere with the passive sensors. Traditional interferers are links of the Fixed Service and of the Inter-Satellites Service. The deployment of systems of the ISS (Inter-Satellite Service) is likely to be feasible, pending the availability of appropriate technology. The author considers it more doubtful for systems of the Fixed Service due to the extremely high linear absorption at ground level. However, potential interference from links of the ISS and from other services generically designed as « Active Terrestrial Service » are considered in the study. For that reason it will be assumed that **each interfering service may be allowed to produce interference level at 3 dB below the interference thresholds indicated in the table 3.2.**

## 4.0 : POTENTIAL INTERFERENCE TO THE LIMB SOUNDERS

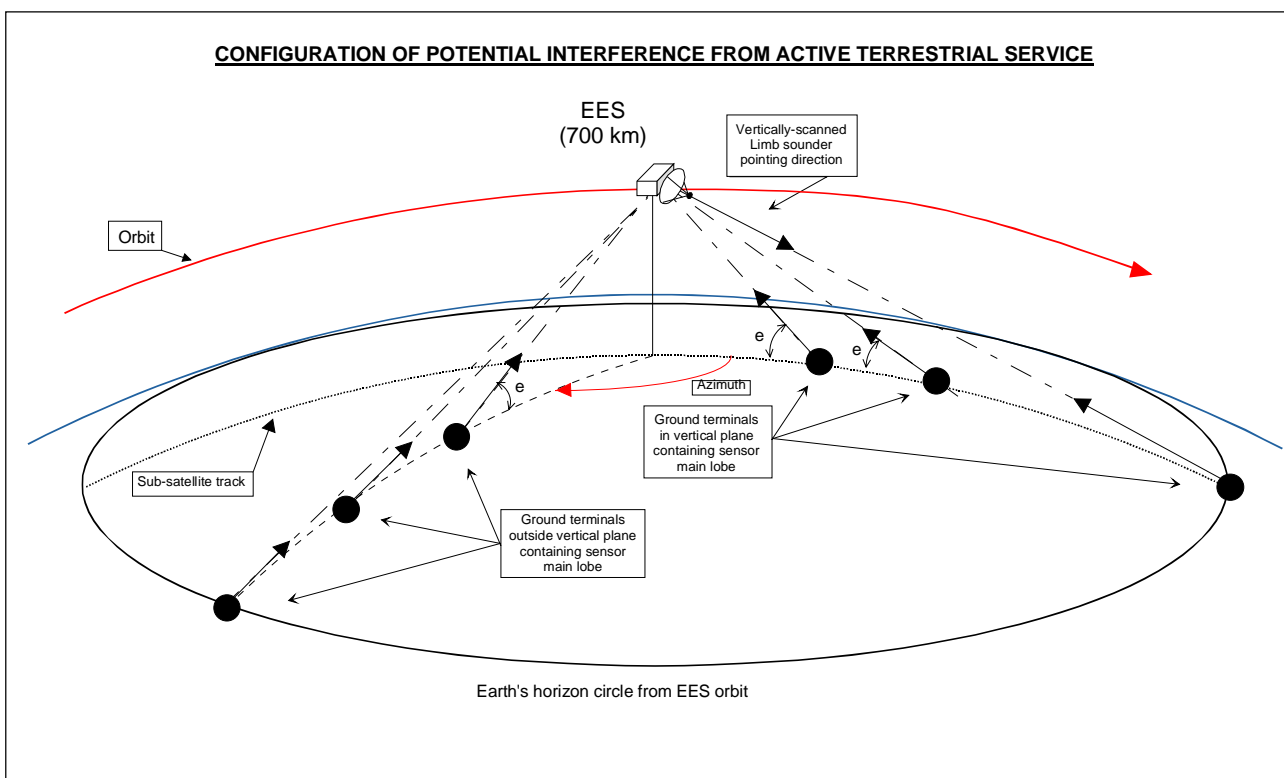
### 4.1 : Budget of potential interference from the Active Terrestrial Service :

#### 4.1.1 : **Geometry of interference :**

It is assumed that the sensor antenna is pointing tangentially to the earth's surface (worst case) and can suffer direct interference from any ground transmitter located on the visible part of the earth's surface. It is further assumed that the interferences can occur via direct links between ground transmitters and the passive sensor antenna. The configuration used for the evaluation is described on the *Figure 4.1.1*. Two cases are considered :

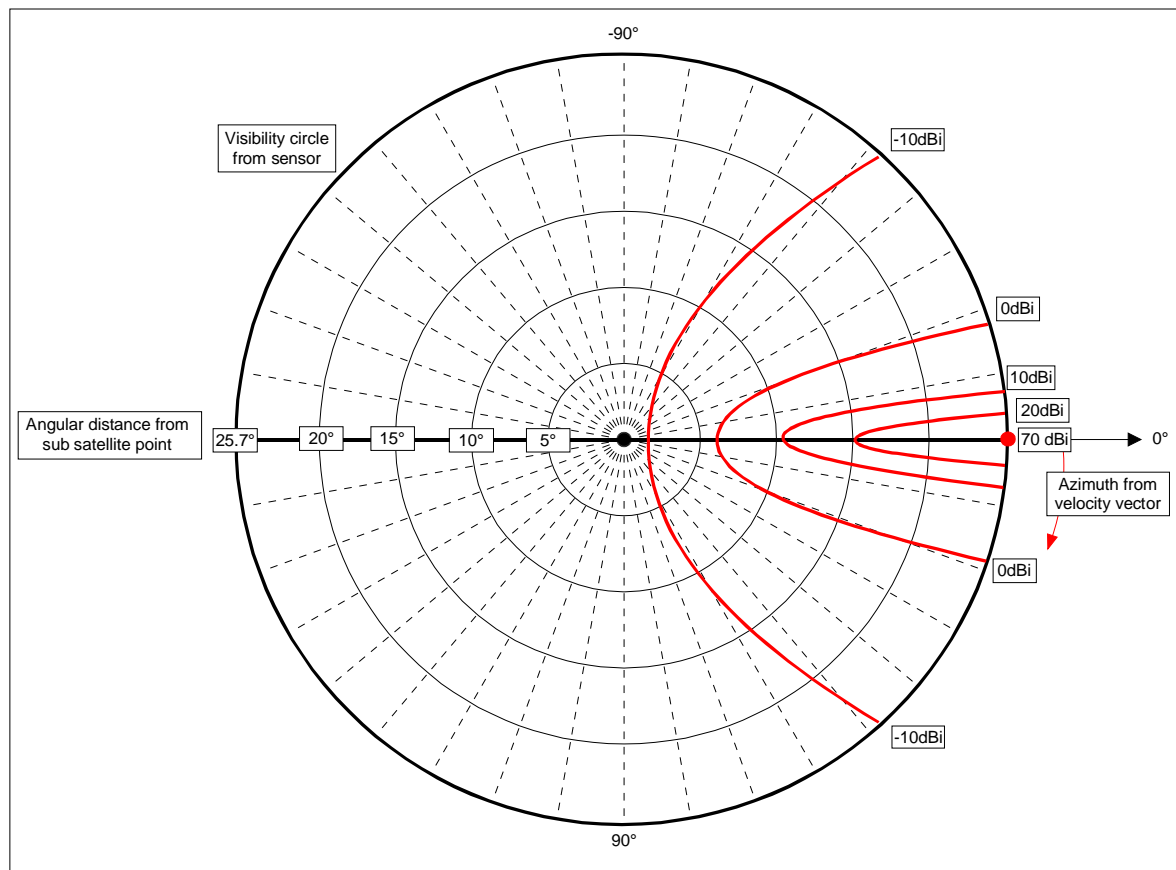
- *Case 1* : The ground transmitter is located in the scanning plane (vertical) of the sensor, and in the direction of sounding (Azimuth close to  $0^\circ$  as referred to the scanning plane/maximum gain direction). Depending on its distance to the sub-satellite point, a ground transmitter "sees" the sensor under various elevation angles from  $0^\circ$  to  $90^\circ$ . Interfering signal can then enter the sensor antenna via its main-lobe when the sensor is seen from the ground transmitter at  $0^\circ$  elevation angle. For increasing elevation angles, interfering signal progressively leaves the sensor's main lobe and can enter the sensor only via its secondary or far lobes;
- *Case 2* : When the azimuth of the fixed terminal is  $\neq 0^\circ$  (outside the scanning plane), the interfering signal can enter the sensor only via its secondary or far lobes.

Figure 4.1.1 : Geometry of potential interference from active terrestrial service



Assuming a 70 dBi gain antenna complying with the recommendation ITU-R F.699-4 pointing tangentially to the earth's surface, the *Figure 4.1.2* shows approximately the iso-gain curves of the sensor's antenna as projected on the visibility circle of the sensor, depending on the azimuth and on the geocentric angular distance to the SSP (Sub-Satellite Point). This represents the gain of the sensor antenna in direction of any potential interferer located in the visibility circle of the passive sensor. Note the forward zone of the visibility circle within the  $-10$  dBi limit of the theoretical far/back lobes, and the considerable increase of the vulnerability to interferences from ground transmitters located in the forward direction (Azimuth approximately  $\pm 48^\circ$ ).

Figure 4.1.2 : Iso-gain lines of the sensor's antenna, projected on the earth's surface



#### 4.1.2 : Maximum acceptable interfering power density

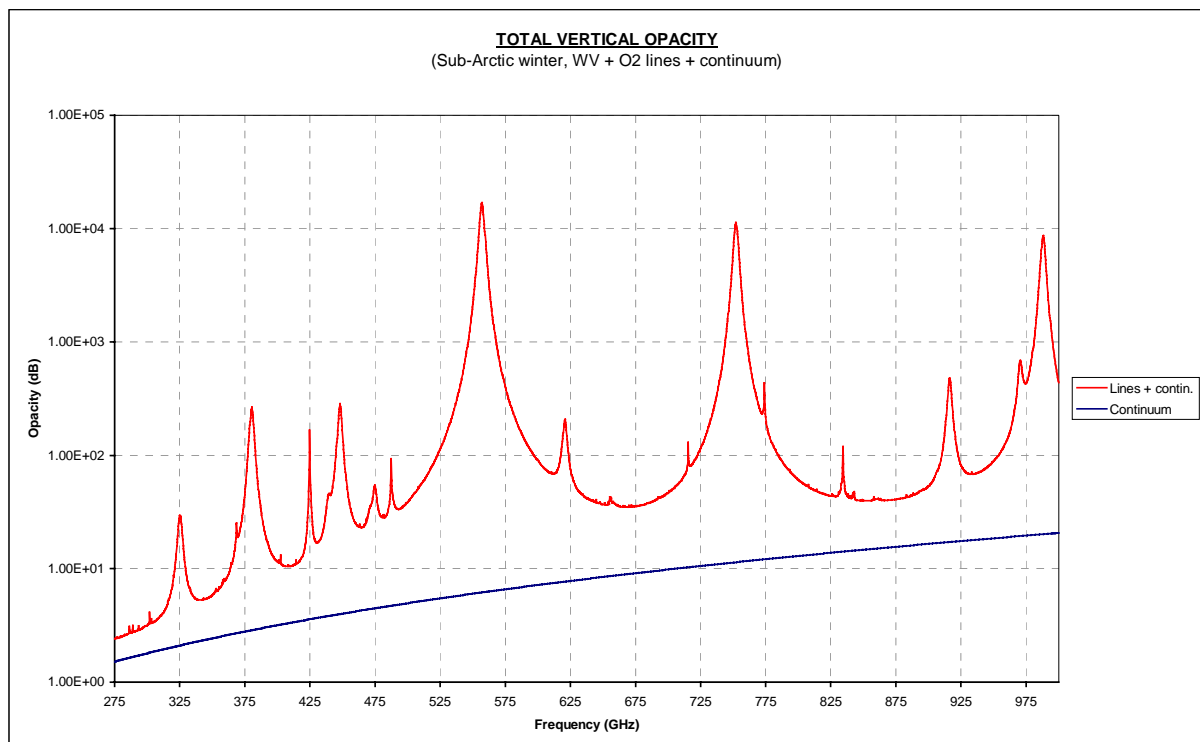
The link budget between the passive sensor and a potential interferer located on the earth's surface is established in the various configurations to evaluate the maximum acceptable EIRP density (Equivalent Isotropic Radiated Power) which does not exceed the interference threshold of the sensor. This involves the following parameters :

##### 4.1.2.1 : Atmosphere model

In case of interference produced by terrestrial services, the atmosphere which absorbs partly the unwanted signals plays a significant role. In the frequency range considered, absorption by water vapour is the dominant factor, and the moisture content is a highly variable parameter which depends on the local climate and seasonal conditions. Because the passive sensors must be operated worldwide, the « Sub-Arctic Winter » atmosphere, where the average humidity content is the lowest and which therefore provides the lowest protection against up-welling interference, is selected for this evaluation.

The *Figure 4.1.3* shows the vertical opacity due to water vapour lines, oxygen lines and continuum. The total continuum is indicated only for reference, showing that the absorption is essentially due to H<sub>2</sub>O resonances. Note the steep increase of average opacity with frequency.

**Figure 4.1.3** : Vertical opacity due to H<sub>2</sub>O+O<sub>2</sub> lines and wet+dry continuum



Considering that frequency allocations for limb sounding, in general, avoid the strong absorption peaks (essentially H<sub>2</sub>O) and are mostly located in the « valleys » between absorption peaks (re.figure 2.2), the analysis are made in three spectral regions which contain most of the bands required for limb sounding, where the vertical opacity is (in a first step) considered constant :

- ✕ **275-375 GHz**, where a vertical opacity equal to **2.4 dB** is adopted;
- ✕ **475-750 GHz**, where a vertical opacity equal to **35 dB** is adopted ;
- ✕ **775-1000 GHz**, where a vertical opacity equal to **40 dB** is adopted.

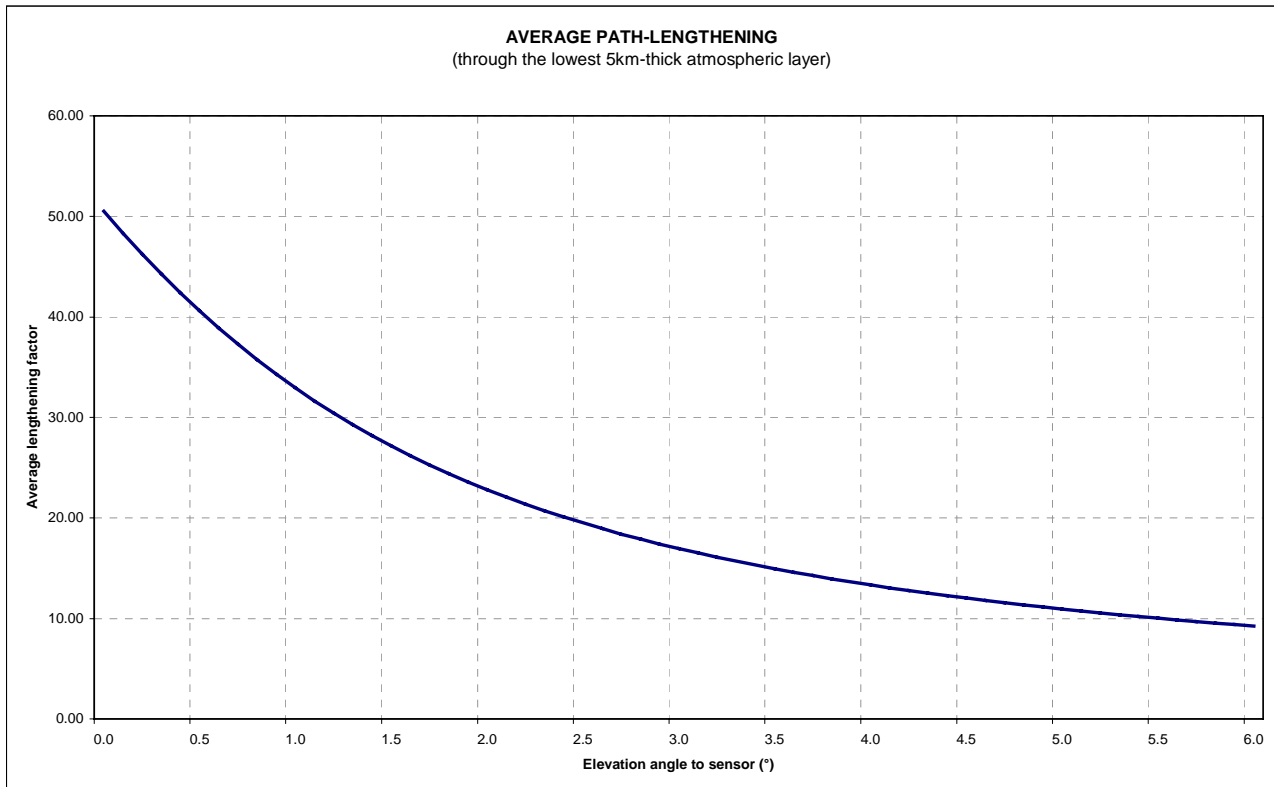
*4.1.2.2 : Atmospheric absorption depending on elevation angle of the interfering path :*

The absorption due to the atmosphere is minimum for a vertical link (the elevation angle ( $\epsilon$ ) is 90°) because in this configuration, the path through the atmosphere is the shortest. For elevation angles lower than 90°, the path length through the atmosphere increases and the absorption increases proportionally. This purely geometric effect is particularly significant for tangential paths at elevation angles close to 0° in the lowest atmospheric layers.

To evaluate the absorption in case of elevation angles different from 90°, it is therefore necessary to take into account a « lengthening factor ». It can be demonstrated that this lengthening factor varies with 1/Sin( $\epsilon$ ) for elevation angles down to 6° ; A more complex calculation is necessary however, for elevation angles between 6 and 0° ; this was done for the lowest 5 km-thick atmospheric layer, assuming that the water vapour is concentrated in this layer. The result is shown on *Figure 4.1.4*.



Figure 4.1.4 : Average lengthening factor for the lowest 5 km-thick atmospheric layer



#### 4.1.2.3 : Path loss depending on elevation angle of the interfering path

The path loss between a ground transmitter and the sensor depending on the elevation angle includes the spreading loss (free space propagation parameter independent from the frequency) and the absorption due to the atmosphere which is frequency dependent. The spreading loss (SL, elevation angle dependant) is computed using the following formula :

$$\text{Spreading loss (SL)} = 4.\pi.D^2$$

$$\text{SL (dB.m}^{-2}\text{)} = 10*\text{Log}(4.\pi.D^2)$$

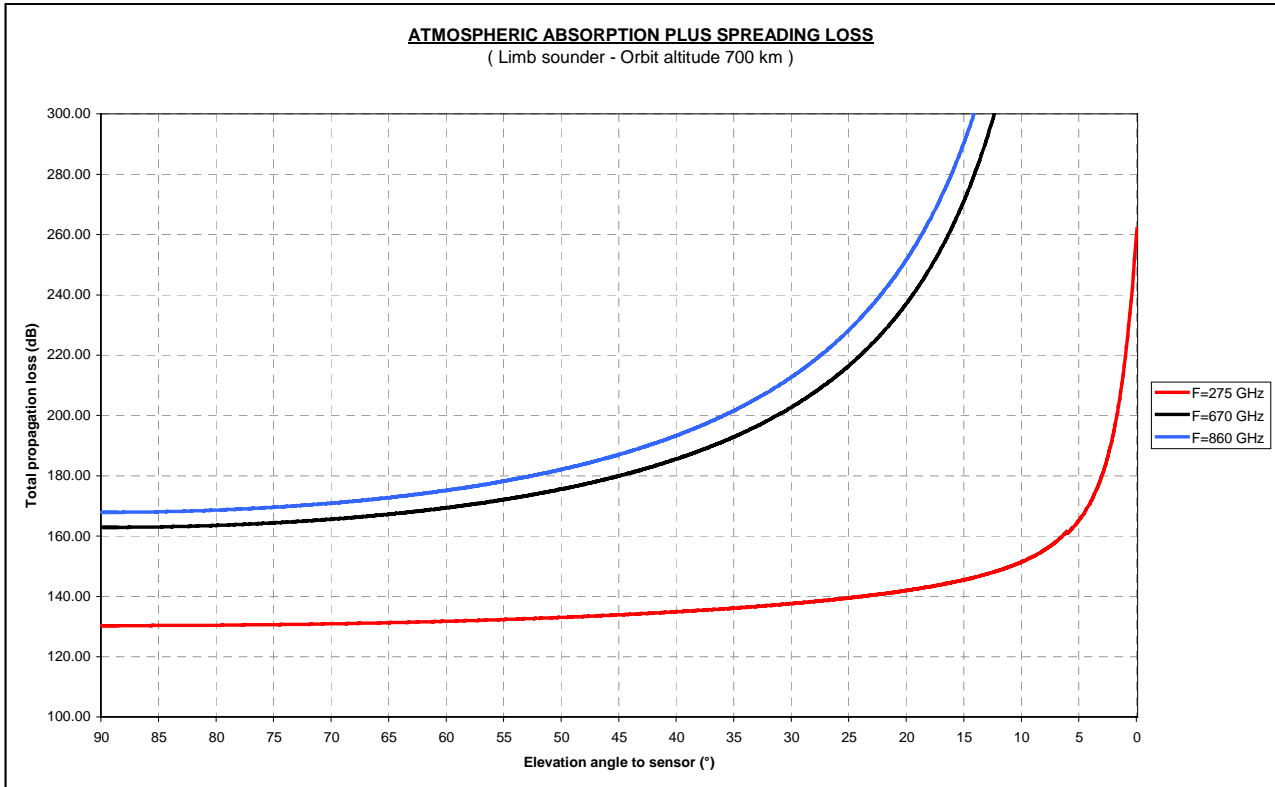
Where D (elevation angle dependant) is the distance between the ground transmitter and the sensor.

The path loss is then given by the formula :

$$\text{Path loss (dB.m}^2\text{)} = \text{SL (dB.m}^2\text{)} + \text{Atm.abs.(dB)}$$

Assuming that the orbit altitude is 700 km, the results are shown on the *Figure 4.1.5*. The total loss increases dramatically for low elevation angles, due to the lengthening factor which affects the lowest atmospheric layers where the absorption is the strongest.

Figure 4.1.5 : Total propagation losses between the earth's surface and the sensor



4.1.2.4 : Effective area of the sensor antenna in direction of the earth's surface

The effective area of the sensor antenna in direction of the earth's surface is computed in the vertical plane which contains the main axis of the antenna. This requires the determination of the angular discrimination between the sensor antenna main axis and the earth's surface depending on the elevation angle, and an antenna model. For that purpose, the antenna model ITU-R F.699-4 was selected. The effective area (elevation angle dependent) is expressed by the formula :

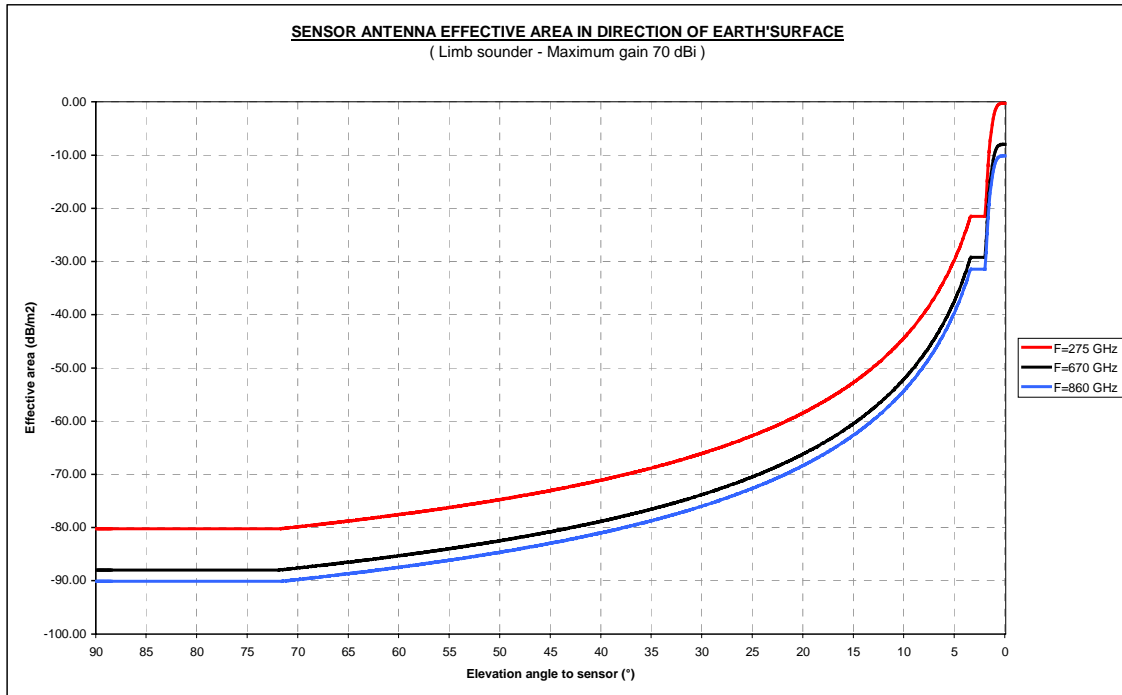
$$\text{Effective area} = \lambda^2 \cdot G / 4 \cdot \pi$$

$$\text{Eff.area (dB.m}^2\text{)} = G \text{ (dB)} + 10 \cdot \text{Log}(\lambda^2 / 4 \cdot \pi)$$

Where  $\lambda$  is the wavelength and G is the isotropic gain in the direction considered.

The effective area is shown on the *Figure 4.1.6*.

Figure 4.1.6 : Sensor antenna effective area in direction of the earth's surface



#### 4.1.2.5 : Maximum acceptable EIRP density in direction of the sensor

The maximum acceptable EIRP density in direction of the sensor is then computed depending on the required radiometric performance and on the position of the interferer in the visibility circle of the sensor. This latter parameter is very important, due to the specific operational configuration of limb sounders which, in certain circumstances, renders possible interference via the main lobe or first side lobes of the sensor's antenna (re.Figure 4.1.2). The following configurations are considered :

- ✘ Two azimuths (**0° and 90°**) and elevation angles ranging from **0° to 90°** are considered ;
- ✘ Three values of the radiometric resolution  $\Delta T_e = 0.1 / 0.01 / 0.001 \text{ K}$  are taken into account with their corresponding interference thresholds **-189 / -199 / -209 dBW/MHz** respectively (re.table 3.2).

The maximum allowable EIRP density is expressed by the formula :

$$\text{EIRP (dBW/MHz)} = \text{Int.thresh.(dBW/MHz)} - \text{Eff.area (dB.m}^2\text{)} + \text{Path loss (dB.m}^{-2}\text{)}$$

This calculation uses the total path loss and the antenna effective area determined in sections 4.1.2.3 & 4.1.2.4. It must be emphasized that «Maximum acceptable EIRP density » means that one single terminal transmitting this EIRP density in the receiver bandwidth of the sensor actually reaches the interference threshold of the sensor. The results are shown on figures 4.1.7, 4.1.8 and 4.1.9 for frequencies 275, 670 and 860 GHz respectively. A summary of the spread sheet showing the numerical results for low elevation angles is given in the Table 4.1.1. Two families of curves are presented, for azimuth 0° where the potential interfering ground transmitter is located in the scanning plane (vertical) of the sensor (Case 1), and for azimuth 90° (Case 2) respectively. Intermediate cases for varying azimuth between 0° and 90° will not be processed individually ; they will receive global attention, based on the interpretation of the figure 4.1.2.

Table 4.1.1 : Maximum EIRP density (dBW/MHz) at low elevation angles

EI.(°)	275 GHz						670 GHz						860 GHz					
	Azimuth 0°			Azimuth 90°			Azimuth 0°			Azimuth 90°			Azimuth 0°			Azimuth 90°		
	0.1 K	0.01 K	0.001 K	0.1 K	0.01 K	0.001 K	0.1 K	0.01 K	0.001 K	0.1 K	0.01 K	0.001 K	0.1 K	0.01 K	0.001 K	0.1 K	0.01 K	0.001 K
18.00	11.00	1.00	-9.00	34.88	24.88	14.88	124.23	114.23	104.23	148.11	138.11	128.11	142.58	132.58	122.58	166.46	156.46	146.46
17.50	10.79	0.79	-9.21	35.22	25.22	15.22	126.93	116.93	106.93	151.37	141.37	131.37	145.73	135.73	125.73	170.17	160.17	150.17
17.00	10.56	0.56	-9.44	35.58	25.58	15.58	129.80	119.80	109.80	154.82	144.82	134.82	149.07	139.07	129.07	174.09	164.09	154.09
16.50	10.33	0.33	-9.67	35.95	25.95	15.95	132.85	122.85	112.85	158.47	148.47	138.47	152.63	142.63	132.63	178.24	168.24	158.24
16.00	10.10	0.10	-9.90	36.34	26.34	16.34	136.11	126.11	116.11	162.34	152.34	142.34	156.42	146.42	136.42	182.65	172.65	162.65
15.50	9.87	-0.13	-10.13	36.74	26.74	16.74	139.59	129.59	119.59	166.47	156.47	146.47	160.47	150.47	140.47	187.34	177.34	167.34
15.00	9.63	-0.37	-10.37	37.17	27.17	17.17	143.32	133.32	123.32	170.86	160.86	150.86	164.81	154.81	144.81	192.35	182.35	172.35
14.50	9.39	-0.61	-10.61	37.62	27.62	17.62	147.32	137.32	127.32	175.55	165.55	155.55	169.46	159.46	149.46	197.69	187.69	177.69
14.00	9.14	-0.86	-10.86	38.09	28.09	18.09	151.63	141.63	131.63	180.58	170.58	160.58	174.47	164.47	154.47	203.41	193.41	183.41
13.50	8.89	-1.11	-11.11	38.58	28.58	18.58	156.27	146.27	136.27	185.97	175.97	165.97	179.86	169.86	159.86	209.55	199.55	189.55
13.00	8.64	-1.36	-11.36	39.11	29.11	19.11	161.30	151.30	141.30	191.77	181.77	171.77	185.69	175.69	165.69	216.16	206.16	196.16
12.50	8.39	-1.61	-11.61	39.67	29.67	19.67	166.75	156.75	146.75	198.02	188.02	178.02	192.02	182.02	172.02	223.29	213.29	203.29
12.00	8.14	-1.86	-11.86	40.27	30.27	20.27	172.67	162.67	152.67	204.80	194.80	184.80	198.89	188.89	178.89	231.02	221.02	211.02
11.50	7.89	-2.11	-12.11	40.90	30.90	20.90	179.15	169.15	159.15	212.15	202.15	192.15	206.39	196.39	186.39	239.40	229.40	219.40
11.00	7.65	-2.35	-12.35	41.59	31.59	21.59	186.24	176.24	166.24	220.17	210.17	200.17	214.61	204.61	194.61	248.54	238.54	228.54
10.50	7.41	-2.59	-12.59	42.32	32.32	22.32	194.04	184.04	174.04	228.95	218.95	208.95	223.64	213.64	203.64	258.55	248.55	238.55
10.00	7.19	-2.81	-12.81	43.12	33.12	23.12	202.66	192.66	182.66	238.59	228.59	218.59	233.62	223.62	213.62	269.55	259.55	249.55
9.50	6.97	-3.03	-13.03	43.98	33.98	23.98	212.23	202.23	192.23	249.24	239.24	229.24	244.69	234.69	224.69	281.70	271.70	261.70
9.00	6.78	-3.22	-13.22	44.93	34.93	24.93	222.91	212.91	202.91	261.06	251.06	241.06	257.04	247.04	237.04	295.19	285.19	275.19
8.50	6.61	-3.39	-13.39	45.98	35.98	25.98	234.90	224.90	214.90	274.27	264.27	254.27	270.90	260.90	250.90	310.26	300.26	290.26
8.00	6.48	-3.52	-13.52	47.13	37.13	27.13	248.46	238.46	228.46	289.11	279.11	269.11	286.55	276.55	266.55	327.20	317.20	307.20
7.50	6.40	-3.60	-13.60	48.43	38.43	28.43	263.90	253.90	243.90	305.92	295.92	285.92	304.37	294.37	284.37	346.39	336.39	326.39
7.00	6.39	-3.61	-13.61	49.88	39.88	29.88	281.62	271.62	261.62	325.12	315.12	305.12	324.82	314.82	304.82	368.31	358.31	348.31
6.50	6.46	-3.54	-13.54	51.54	41.54	31.54	302.18	292.18	282.18	347.26	337.26	327.26	348.51	338.51	328.51	393.59	383.59	373.59
6.00	5.90	-4.10	-14.10	52.69	42.69	32.69	315.17	305.17	295.17	361.97	351.97	341.97	363.59	353.59	343.59	410.39	400.39	390.39
5.50	6.05	-3.95	-13.95	54.71	44.71	34.71	340.64	330.64	320.64	389.31	379.31	369.31	392.94	382.94	372.94	441.61	431.61	421.61
5.00	6.35	-3.65	-13.65	57.06	47.06	37.06	370.72	360.72	350.72	421.44	411.44	401.44	427.59	417.59	407.59	478.30	468.30	458.30
4.50	6.84	-3.16	-13.16	59.82	49.82	39.82	406.68	396.68	386.68	459.66	449.66	439.66	468.99	458.99	448.99	521.97	511.97	501.97
4.00	7.61	-2.39	-12.39	63.13	53.13	43.13	450.26	440.26	430.26	505.79	495.79	485.79	519.13	509.13	499.13	574.66	564.66	554.66
3.50	8.74	-1.26	-11.26	67.15	57.15	47.15	503.90	493.90	483.90	562.31	552.31	542.31	580.82	570.82	560.82	639.23	629.23	619.23
3.00	13.40	3.40	-6.60	72.13	62.13	52.13	574.05	564.05	554.05	632.77	622.77	612.77	661.02	651.02	641.02	719.74	709.74	699.74
2.50	19.69	9.69	-0.31	78.41	68.41	58.41	663.55	653.55	643.55	722.27	712.27	702.27	763.28	753.28	743.28	822.01	812.01	802.01
2.00	27.77	17.77	7.77	86.50	76.50	66.50	779.36	769.36	759.36	838.08	828.08	818.08	895.61	885.61	875.61	954.34	944.34	934.34
1.50	24.15	14.15	4.15	97.09	87.09	77.09	917.50	907.50	897.50	990.44	980.44	970.44	1055.49	1045.49	1035.49	1128.44	1118.44	1108.44
1.00	32.52	22.52	12.52	111.12	101.12	91.12	1114.25	1104.25	1094.25	1192.85	1182.85	1172.85	1281.14	1271.14	1261.14	1359.74	1349.74	1339.74
0.50	49.74	39.74	29.74	129.65	119.65	109.65	1381.02	1371.02	1361.02	1460.93	1450.93	1440.93	1586.18	1576.18	1566.18	1666.10	1656.10	1646.10
0.00	73.61	63.61	53.61	153.61	143.61	133.61	1728.28	1718.28	1708.28	1808.28	1798.28	1788.28	1983.04	1973.04	1963.04	2063.04	2053.04	2043.04

### 4.1.3 : Results of the simulation (Figures 4.1.7, 4.1.8, 4.1.9)

#### 4.1.3.1 : General remarks

In all cases, the acceptable EIRP density increases with the frequency ; due to the augmentation of propagation loss and atmospheric absorption.

There is a significant increase of the acceptable EIRP density near 0° elevation, due to the atmospheric absorption considerably augmented by the « lengthening factor » at grazing angles :

- ✘ **At 275 GHz** (Figure 4.1.7), the atmospheric absorption is low. The vertical opacity is 2.4 dB only. As a consequence, the effect of the high gain sensor's antenna in the forward direction (re. Figure 4.1.2) is predominant and is clearly visible on the curves representing the « Azimuth 0° case », which are significantly depressed between elevation angles 3° and 60° corresponding to the theoretical first secondary lobes region of the sensor's antenna.
- ✘ **At frequencies 670 and 860 GHz** (figures 4.1.8 & 4.1.9), the atmospheric absorption is high. The vertical opacities are 35 and 40 dB respectively. In consequence, the effect of the sensor's antenna gain in the forward direction is very largely compensated by the atmospheric absorption at all elevation angles (re. Figure 4.1.5). The maximum acceptable EIRP density is extremely high near 0° elevation, and decreases progressively for increasing elevation angle. There is not much difference between the « Azimuth 0° » and the « Azimuth 90° » curves. These cases are not considered critical.

#### 4.1.3.2 : Discussions of the results

**The situation at 275 GHz is clearly the most critical.** The discussion below concentrates mainly on this case.

Figure 4.1.7 : Maximum EIRP density around 275 GHz

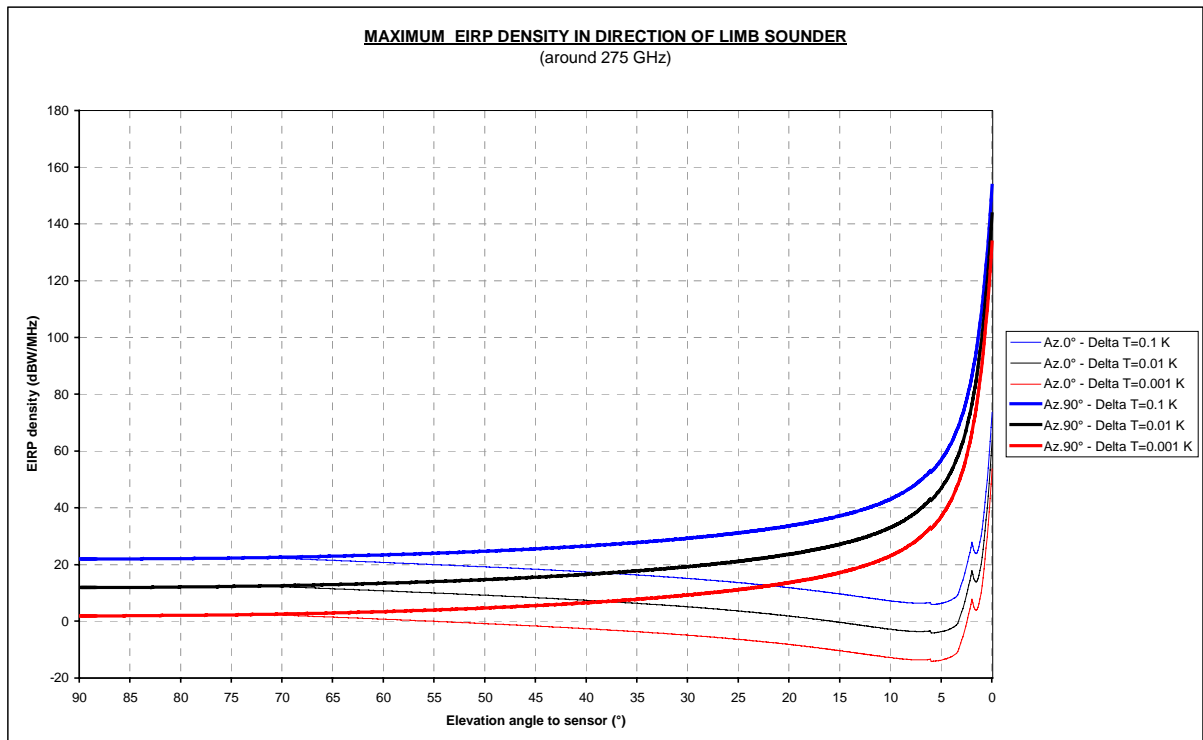


Figure 4.1.8 : Maximum EIRP density around 670 GHz

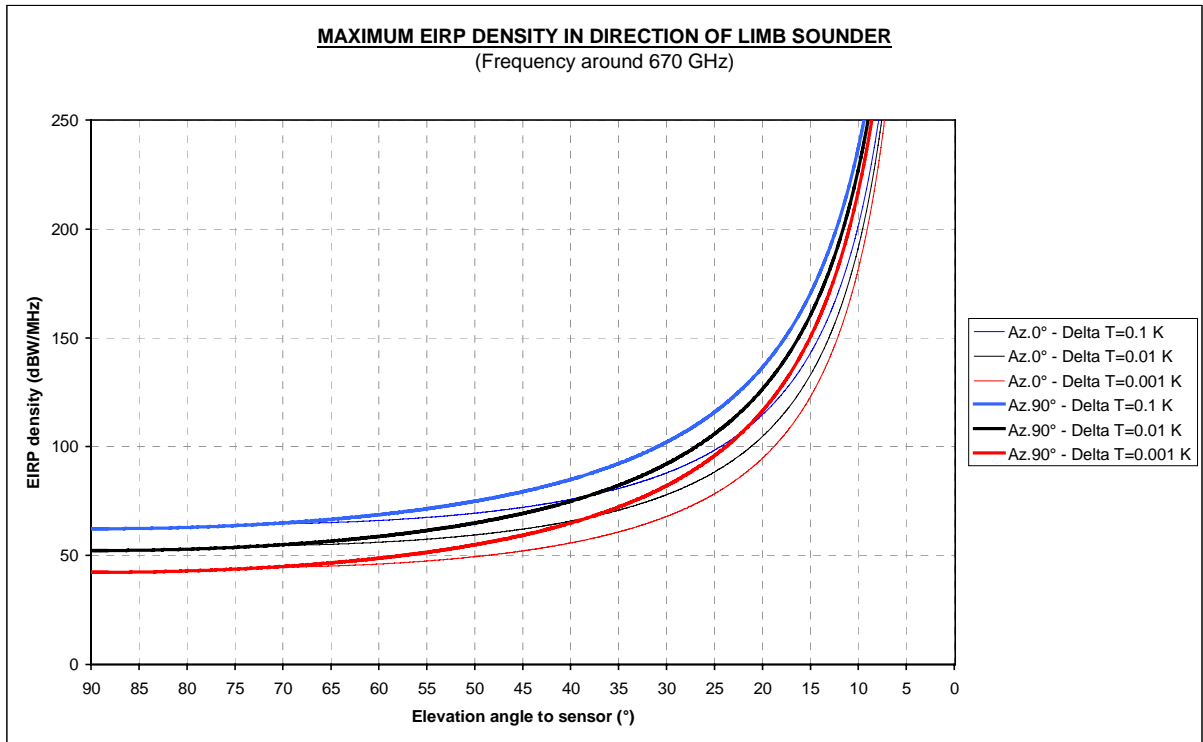
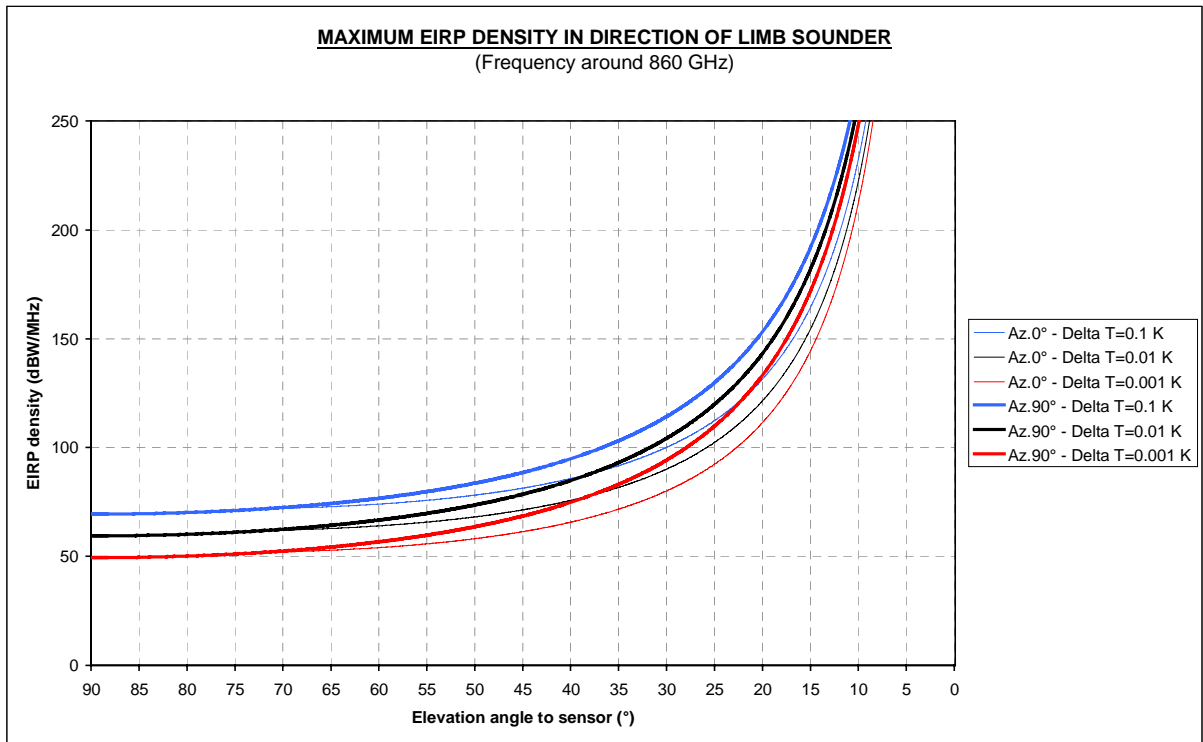


Figure 4.1.9 : Maximum EIRP density around 860 GHz



- ✘ **Maximum acceptable EIRP density in direction of the sensor from ground transmitters which are very close to the sub-satellite track at very low elevation angles** can reach 54 dBW/MHz (for  $\Delta T = 0.001$  K). The criticality of this potential threat depends on the population of ground transmitters which are located inside the sensor's antenna foot print on the earth's surface therefore on the size of this foot-print, and on the probability of several ground transmitters pointing in the direction of the passive sensor in a main lobe to main lobe configuration.

For the 70 dBi gain antenna adopted in this analysis, and relying on the antenna pattern such as defined in the recommendation ITU-R F.699-4, the approximate dimensions of the sensor antenna main lobe foot-print on the earth's surface are given in the Table 4.1.2. It is noted that the isotropic gain at the edge of the foot-print is 21 dB below the maximum.

Table 4.1.2 : Foot-print of the passive sensor antenna at grazing angle

	Width	Along track foot-print	Cross track foot-print	Area
<b>Main lobe</b>	0.15°	500 km	8 km	4000 km <sup>2</sup>
<b>Half-power lobe</b>	0.054°	280 km	3 km	840 km <sup>2</sup>

Of course, the characteristics of ground transmitters of the « Active terrestrial service » are, and will certainly be for a while, unknown. However, assuming an important population of such hypothetical terminals concentrated within this foot-print and considering also the technological limitations and the low probability of several main-lobe to main-lobe occurrences, it seems very unlikely that the aggregate of their contributions can reach the 54 dBW/MHz upper limit. The problem is not there.

- ✘ **Interference from ground transmitters which are anywhere within the visibility circle of the sensor, except at azimuth within +/- 48°** (re.Figure 4.1.2), can occur via the far lobes only of the sensor's antenna. The maximum acceptable EIRP density is very high at 0° elevation angle and decreases regularly at increasing elevation angle (re.Figure 4.1.7, Az.90° case).
- ✘ **In the intermediate case, when the ground transmitters are located at azimuth within +/- 48°** (re.Figure 4.1.2), the interference can occur via the first secondary lobes of the sensor's antenna, where the isotropic gain is still high. Curves representing the maximum acceptable EIRP density were not computed, but they will obviously fill the gap between Az.0° and Az.90° cases on the Figure 4.1.7.
- ✘ **To simplify the applicability of possible constraints on the « Active terrestrial service » worldwide**, it seems essential to define a unique global EIRP density threshold for all elevation angles and at all azimuths. The Figure 4.1.7 suggests a possible solution : Above a certain elevation angle ( about 3° in case of the Figure 4.1.7 ), there is an horizontal symmetry between *Azimuth 0°* and *Azimuth 90°* curves, suggesting that an average value would be a fair compromise between the corresponding higher and lower susceptibilities to interference. Averaging the Az.0° and Az.90° curves for each value of  $\Delta T_e$  leads to a set of 3 EIRP densities which are applicable to any elevation angle above a certain value. The *Table 4.1.3* proposes such limits which depend on the frequency and on the  $\Delta T_e$  requirement, as derived from figure 4.1.7. Limits derived from the higher frequency cases (figures 4.1.8 & 4.1.9) are also presented.

Because these limits represent the total acceptable contribution which is the aggregate of all single-entry contributions, they must further be apportioned among the possible population of ground transmitters within the visibility circle of the passive sensor. The Table 4.1.3 also indicates the size of the visibility circle, which is an important parameter for the evaluation of the population of ground transmitters.

**Table 4.1.3 : Proposed Global EIRP density limits**

<b>Frequency range (GHz) :</b>	<b>275-375</b>	<b>475-750</b>	<b>775-1000</b>
<b>EIRP density limit (dBW/MHz)</b>			
For $\Delta T = 0.1$ K :	22	62	69
For $\Delta T = 0.01$ K :	12	52	59
For $\Delta T = 0.001$ K :	2	42	49
<b>Geometric parameters</b>			
Range of Elevation (°):	3 to 90	20 to 90	20 to 90
Visib.circle radius (km) :	2540	1345	1345
Visib.circle area (km <sup>2</sup> ) :	20 million	5.7 million	5.7 million

Very large regions are visible from the passive sensor. It is reasonable to assume, for instance in densely populated western Europe, that 80 medium to large towns (100 km<sup>2</sup> in average) can be simultaneously visible. Ground links operating in this frequency range are unknown, but assuming, in each town, a density of 2 links/km<sup>2</sup> in the lowest part of the frequency range where the linear absorption (excluding absorption lines) is not very high, 16000 terminals can simultaneously interfere with the passive sensor. Above 475 GHz where the linear absorption can exceed 50 dB/km (see figure 2.2), a density of 50 and more links/km<sup>2</sup> is considered. Under these assumptions, the Table 4.1.4 below proposes a set of single-entry limitations applicable to any single ground transmitter.

**Table 4.1.4 : Proposed single-entry EIRP density limits applicable to ground transmitters**

<b>Frequency range (GHz) :</b>	<b>275-375</b>	<b>475-750</b>	<b>775-1000</b>
<b>Single entry EIRP density limit (dBW/MHz)</b>			
Range of Elevation (°):	3 to 90	20 to 90	20 to 90
For $\Delta T = 0.1$ K :	-20	6	13
For $\Delta T = 0.01$ K :	-30	-4	3
For $\Delta T = 0.001$ K :	-40	-14	-7

**4.1.3.3 : Preliminary conclusion on co-frequency sharing between limb sounders and the Active terrestrial service**

- ✦ **At frequencies 275-375 GHz**, there is a drastic gap (more than 50 dB) between the maximum EIRP density that would be acceptable at elevation angles below 3° and the limit that would be necessary at elevation angles above 3°. These results were obtained considering that the sensor's antenna is pointing tangentially to the earth's surface, which is the worst case.

If the antenna is pointing at 10 km altitude for instance, the main difference is the augmentation of the acceptable EIRP density at 0° elevation angle by about 20 dB but the vulnerability at higher elevation angles is not significantly reduced.



The confidence in the constraints indicated in the Table 4.1.4 relies on the utilization of high performance antennas by ground transmitters of the active terrestrial service, with steep attenuation of the side-lobe level above 0° elevation angle, and on a very strict control of the pointing direction of these antennas above horizon.

Past experience suggests that such constraints are not practical, in particular because Administrations are not able to monitor the deployment of ground networks in order to verify that the constraints are respected. To obviate the need for such a rigorous control, a unique EIRP density, low enough to be applicable at all elevation angles (re.table 4.1.4) should be adopted. As a consequence it is provisionally concluded that **co-frequency sharing in the 275-375 GHz frequency band is feasible, for any value of the required  $\Delta T_e$ , only if these low EIRP densities are acceptable to the active terrestrial service.**

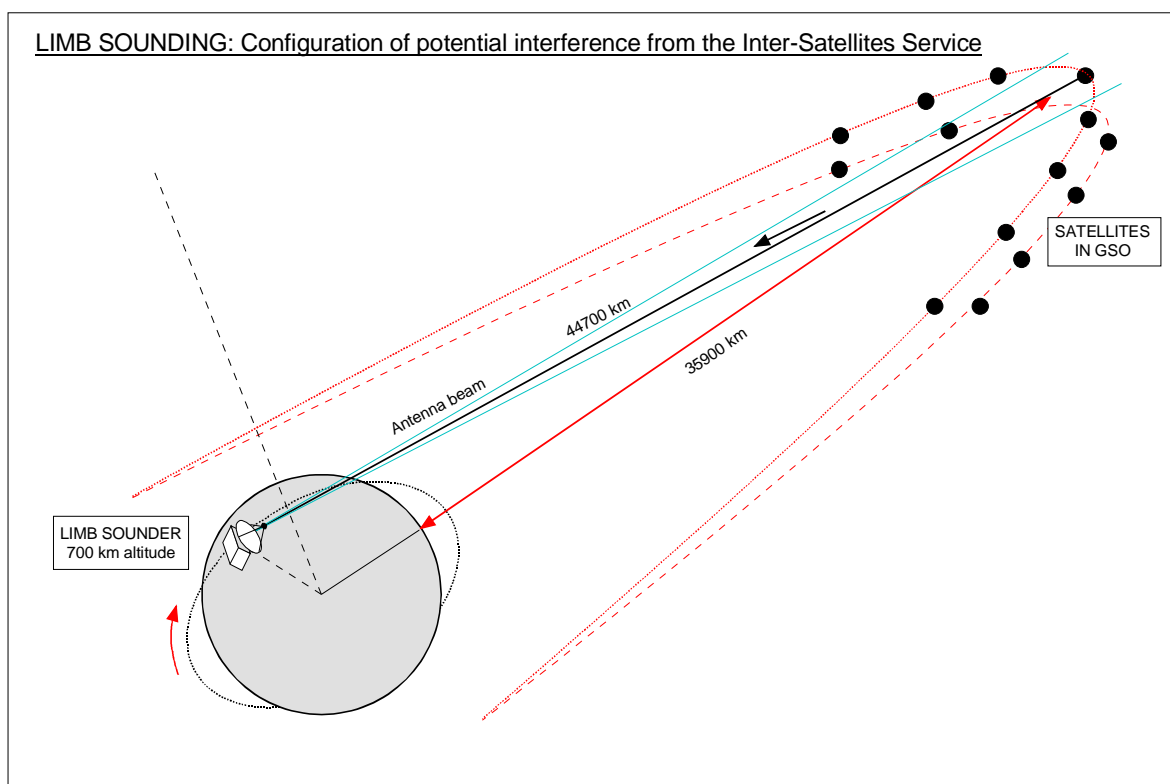
- ✘ **At frequencies 475 to 1000 GHz**, the situation is much less critical. It seems that co-frequency sharing is feasible, and would not place severe constraints, if any, on the active terrestrial service. This conclusion is provisional, pending the availability of detailed terrestrial services objectives and requirements, and appropriate further studies.

#### 4.2 : Budget of potential interference from the Inter-satellites Service :

##### 4.2.1 : Geometry of interference :

The passive sensor antenna is pointing tangentially to atmospheric layers, at altitudes ranging from a few kilometers to more than 100 km. To study potential interference from terrestrial services an altitude of 0km was considered as the worst case. Considering now interference produced by the Inter-Satellites Service, the worst case is where the absorption due to the atmosphere can be neglected, say at altitudes above 50 km where the atmospheric pressure is < 1 hPa. The *figure 4.2.1* describes the geometry of potential interference from Inter-Satellites Service considered in the study.

Figure 4.2.1 : Geometry of potential interference from the Inter-Satellites Service



Past studies on passive sensors in the 60/118/183 GHz frequency range concluded that co-frequency sharing with links of the **ISS in non-geostationary orbits is not feasible** due to the vulnerability of the cold space calibration of the passive sensors. Considering that the configuration of passive sensors around 60/118/183 GHz in cold-space calibration mode and the configuration of limb sounders are similar, and moreover that limb sounders may be more vulnerable due to their higher antenna gain and higher sensitivity, it is considered that :

- ✘ **Co-frequency sharing with links of the ISS between satellites in non-geostationary orbits is not feasible.**
- ✘ As a consequence, the present study considers **exclusively co-frequency sharing with links of the ISS between satellites in geostationary orbit.**

It is noted that the minimum longitudinal separation between satellites of GSO system of the ISS on their common orbit is 1° (long range link), and that several orbits of various inclination angles may also be envisaged.

The main beam of the limb sounder, assumed to be in a low earth inclined orbit, can aim at the geosynchronous orbits two times during each of its orbital period, in the vicinity of the highest latitude attained by the orbit (assuming that the geosynchronous orbits are not too highly inclined).

The consequence is that several satellites of the GSO systems may be simultaneously within the main and first secondary lobes of the limb sounder antenna, and may contribute to the build up of the interference level that is suffered by the sensor.

In the *table 4.2.1*, the potential relative contributions of ISS links which are contained within the main and first secondary lobes of the passive sensor's antenna, are evaluated depending on their angular distance to the maximum gain position. The number of GSO satellites of the ISS is derived from the extremely improbable situation where satellites are placed every degree in longitude and in latitude.

In the table, « Antenna zone » is identified by a range of isotropic gains, « off-set angle » refers to the main axis of the passive sensor antenna and « geocentric angle » refers to the geostationary altitude.

It can be concluded that, despite the very pessimistic assumption concerning the density of satellites of the ISS, the aggregate contributions of ISS links which are not in the maximum gain direction of the passive sensor antenna have a very minor effect and can be neglected. **Single-entry interferences are therefore considered in the study.**

Table 4.2.1 : Relative contribution of ISS links in sensor's antenna main and first secondary lobes

<b>Antenna zone :</b>	70 to 40 dBi	40 to 30 dBi	30 to 20 dBi	20 to 10 dBi
<b>Off-set angle :</b>	0 to 0.5°	0.5 to 1.2°	1.2 to 3°	3 to 7.6°
<b>Antenna beamwidth :</b>	1° at -30 dB	2.4° at -40 dB	6° at -50 dB	15.2° at -60 dB
<b>Geocentric angle :</b>	1° at -30 dB	2.5° at -40 dB	6.3° at -50 dBi	16° at -60 dBi
<b>Potential nb.satellites :</b>	1 at 70dBi	4	24	150
<b>Contrib.re.main lobe :</b>	N/A	-29 dB	-31 dB	-33 dB

#### **4.2.2 : Maximum acceptable single-entry power flux density in the environment of the sensor :**

Links between satellites of an ISS system can aim at almost any position of the geosynchronous orbits that can be used by the ISS. The interfering power received by the passive sensor in low earth orbit (LEO) depends on the distance between each satellite of the ISS and the passive sensor and on the EIRP in direction of the LEO. These are varying parameters which cannot be easily predicted and therefore cannot be converted into a unique sharing criteria applicable to all links of the ISS.

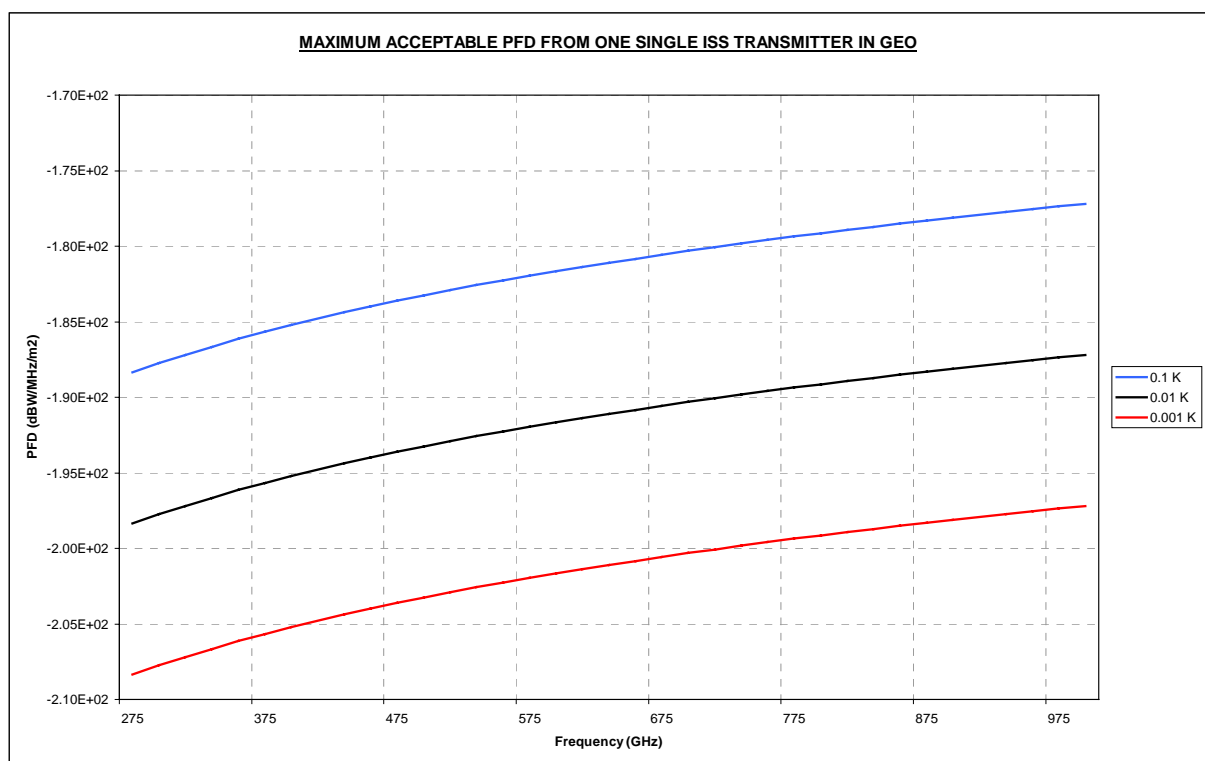
The sharing criteria already adopted in similar sharing situations around 60 GHz, 118 GHz and 183 GHz is the power flux density (PFD) at the level of the passive sensor's antenna, which depends only on the interference threshold of the sensor (re. *table 4.2.2*) and the effective area of its antenna.

Table 4.2.2 : Maximum acceptable contribution of the ISS to the interference threshold

<b>Radiometric resolution :</b>	0.1 K	0.01 K	0.001 K
<b>Contribution of the ISS :</b>	-189 dBW/MHz	-199 dBW/MHz	-209 dBW/MHz

The maximum acceptable single-entry PFD depending on the frequency is presented in a graphic form on the *figure 4.2.2*, for three values of the required  $\Delta T_e$ . Numerical results are shown in the table 4.2.3.

Figure 4.2.2 : Maximum single-entry PFD at the level of the sensor



#### 4.2.3 : Provisional sharing criteria :

Sharing criteria should then be established by associating to the frequency bands listed in the table 2.2 (required for limb sounding) the corresponding PFD upper limit shown on the figure 4.2.2 or tabulated in the table 4.2.3.

However, many frequency bands are proposed in the table 2.2, and considering individually each of them would certainly be a cumbersome exercise. It might be more practical to split the spectral domain of interest (275-1000 GHz) into a limited number of bands, each containing several limb sounding frequencies, where unique PFD limits would apply. In each band, the « unique » PFD limit adopted would be the PFD at the bottom of the band, although it may be considered detrimental to the ISS.

To illustrate this approach, the criteria proposed below is applicable to the limb sounding frequency bands contained within the 275-390 GHz region, and the PFD at 275 GHz applies. The wording is a standard one (re. The 60 GHz case), only the sentences in *italics* (frequency band and PFD) are specific.

Limb sounders of the EESS (Earth Exploration Satellite Service) and inter-satellite links of GSO satellite systems of the ISS can share the same frequency bands in the 275 to 390 GHz spectral region provided that the single-entry power flux-density at all altitudes from 0 to 1000 km above the Earth's surface produced by a station in the inter-satellite service, for all conditions and for all methods of modulation, shall not exceed  $-208 \text{ dBW/MHz/m}^2$  for all angles of arrival.

Table 4.2.3 : Maximum PFD depending on  $\Delta T_e$  and frequency

Freq.(GHz)	Lambda (m)	Ef.area (dB/m2)	p.f.d.(dBW/MHz/m2)		
			0.1 K	0.01 K	0.001 K
275	1.09E-03	-2.36E-01	-1.88E+02	-1.98E+02	-2.08E+02
295	1.02E-03	-8.46E-01	-1.88E+02	-1.98E+02	-2.08E+02
315	9.52E-04	-1.42E+00	-1.87E+02	-1.97E+02	-2.07E+02
335	8.96E-04	-1.95E+00	-1.87E+02	-1.97E+02	-2.07E+02
355	8.45E-04	-2.45E+00	-1.86E+02	-1.96E+02	-2.06E+02
375	8.00E-04	-2.93E+00	-1.86E+02	-1.96E+02	-2.06E+02
395	7.59E-04	-3.38E+00	-1.85E+02	-1.95E+02	-2.05E+02
415	7.23E-04	-3.81E+00	-1.85E+02	-1.95E+02	-2.05E+02
435	6.90E-04	-4.22E+00	-1.84E+02	-1.94E+02	-2.04E+02
455	6.59E-04	-4.61E+00	-1.84E+02	-1.94E+02	-2.04E+02
475	6.32E-04	-4.98E+00	-1.84E+02	-1.94E+02	-2.04E+02
495	6.06E-04	-5.34E+00	-1.83E+02	-1.93E+02	-2.03E+02
515	5.83E-04	-5.69E+00	-1.83E+02	-1.93E+02	-2.03E+02
535	5.61E-04	-6.02E+00	-1.83E+02	-1.93E+02	-2.03E+02
555	5.41E-04	-6.34E+00	-1.82E+02	-1.92E+02	-2.02E+02
575	5.22E-04	-6.64E+00	-1.82E+02	-1.92E+02	-2.02E+02
595	5.04E-04	-6.94E+00	-1.82E+02	-1.92E+02	-2.02E+02
615	4.88E-04	-7.23E+00	-1.81E+02	-1.91E+02	-2.01E+02
635	4.72E-04	-7.51E+00	-1.81E+02	-1.91E+02	-2.01E+02
655	4.58E-04	-7.77E+00	-1.81E+02	-1.91E+02	-2.01E+02
675	4.44E-04	-8.04E+00	-1.81E+02	-1.91E+02	-2.01E+02
695	4.32E-04	-8.29E+00	-1.80E+02	-1.90E+02	-2.00E+02
715	4.20E-04	-8.54E+00	-1.80E+02	-1.90E+02	-2.00E+02
735	4.08E-04	-8.78E+00	-1.80E+02	-1.90E+02	-2.00E+02
755	3.97E-04	-9.01E+00	-1.80E+02	-1.90E+02	-2.00E+02
775	3.87E-04	-9.24E+00	-1.79E+02	-1.89E+02	-1.99E+02
795	3.77E-04	-9.46E+00	-1.79E+02	-1.89E+02	-1.99E+02
815	3.68E-04	-9.67E+00	-1.79E+02	-1.89E+02	-1.99E+02
835	3.59E-04	-9.88E+00	-1.79E+02	-1.89E+02	-1.99E+02
855	3.51E-04	-1.01E+01	-1.79E+02	-1.89E+02	-1.99E+02
875	3.43E-04	-1.03E+01	-1.78E+02	-1.88E+02	-1.98E+02
895	3.35E-04	-1.05E+01	-1.78E+02	-1.88E+02	-1.98E+02
915	3.28E-04	-1.07E+01	-1.78E+02	-1.88E+02	-1.98E+02
935	3.21E-04	-1.09E+01	-1.78E+02	-1.88E+02	-1.98E+02
955	3.14E-04	-1.10E+01	-1.78E+02	-1.88E+02	-1.98E+02
975	3.08E-04	-1.12E+01	-1.77E+02	-1.87E+02	-1.97E+02
995	3.02E-04	-1.14E+01	-1.77E+02	-1.87E+02	-1.97E+02

## 5.0 : POTENTIAL INTERFERENCE TO THE NADIR SOUNDERS

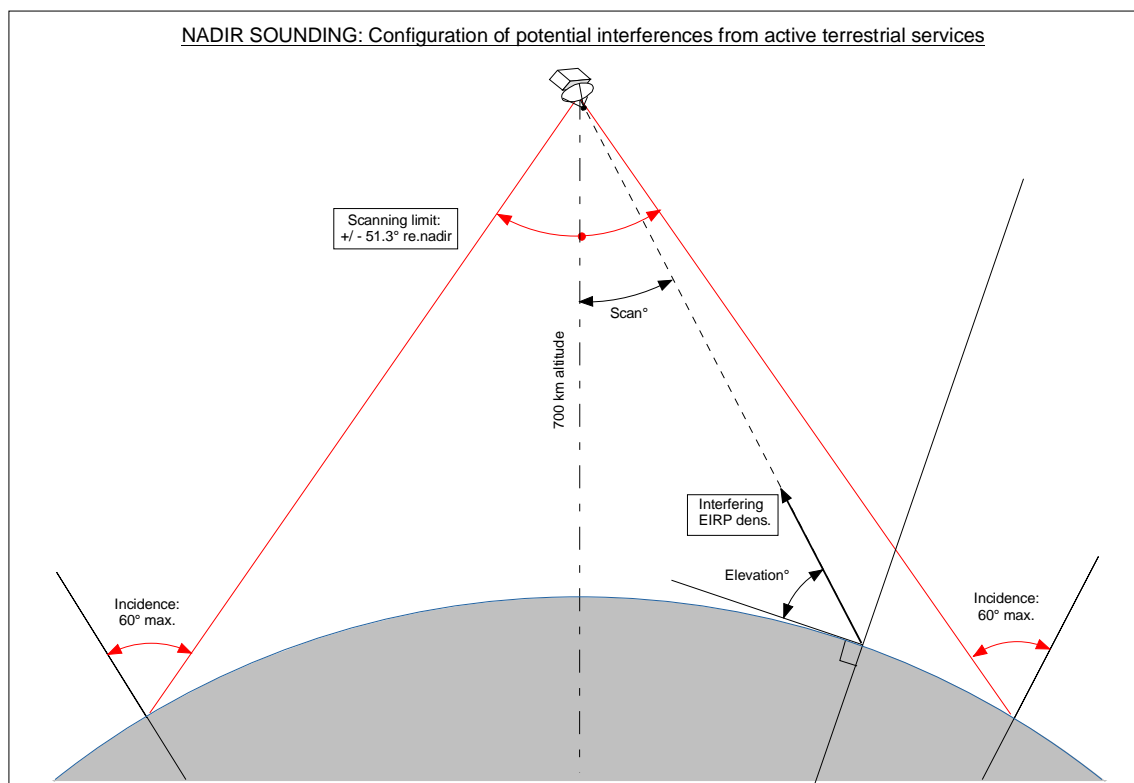
### 5.1 : Budget of potential interference to nadir sounders in LEO from the « Active terrestrial service »

#### 5.1.1 : **Geometry of interference :**

The sensor's antenna is pointing in direction of the earth's surface and is scanned perpendicularly to the orbit plane within  $\pm 51.3^\circ$  re.the nadir direction. The scanning angle is determined in order not to exceed  $60^\circ$  incidence angle at ground level. This configuration is illustrated on the *figure 5.1.1*

The sensor can receive interference essentially via its main lobe, from ground transmitters which are located within the « pixel » of the passive sensor, assumed to be limited by the half-power beamwidth of the antenna. The worst case occurs when the sensor's antenna is pointing in the nadir direction, where the shielding provided by the atmospheric absorption is the lowest.

Figure 5.1.1 : Geometry of potential interference from the Active terrestrial service



#### 5.1.2 : **Maximum acceptable interfering power density**

The link budget between the passive sensor and a potential interferer located on the earth's surface are established in the worst configuration, when the sensor's antenna is pointing in the nadir direction. The maximum acceptable EIRP density will be established, using parameters similar to those already described for the limb sounders case.

##### 5.1.2.1 : *Atmosphere model and frequencies adopted for the simulation*

The absorption conditions which prevail in the « Sub-Arctic winter » atmosphere are adopted for the evaluation.

The frequency allocations for nadir sounding are in most cases selected around  $H_2O$  and  $O_2$  resonances. In addition a number of window channels should also be selected close enough to the resonances, but in regions where the vertical absorption is the lowest possible.

The frequency bands retained for the evaluation are listed in the *table 5.1.1*, as well as the minimum vertical absorption which prevails in each band (the foot of the absorption peak). Some window channels have a question mark because their usefulness may appear questionable considering the magnitude of the vertical absorption.

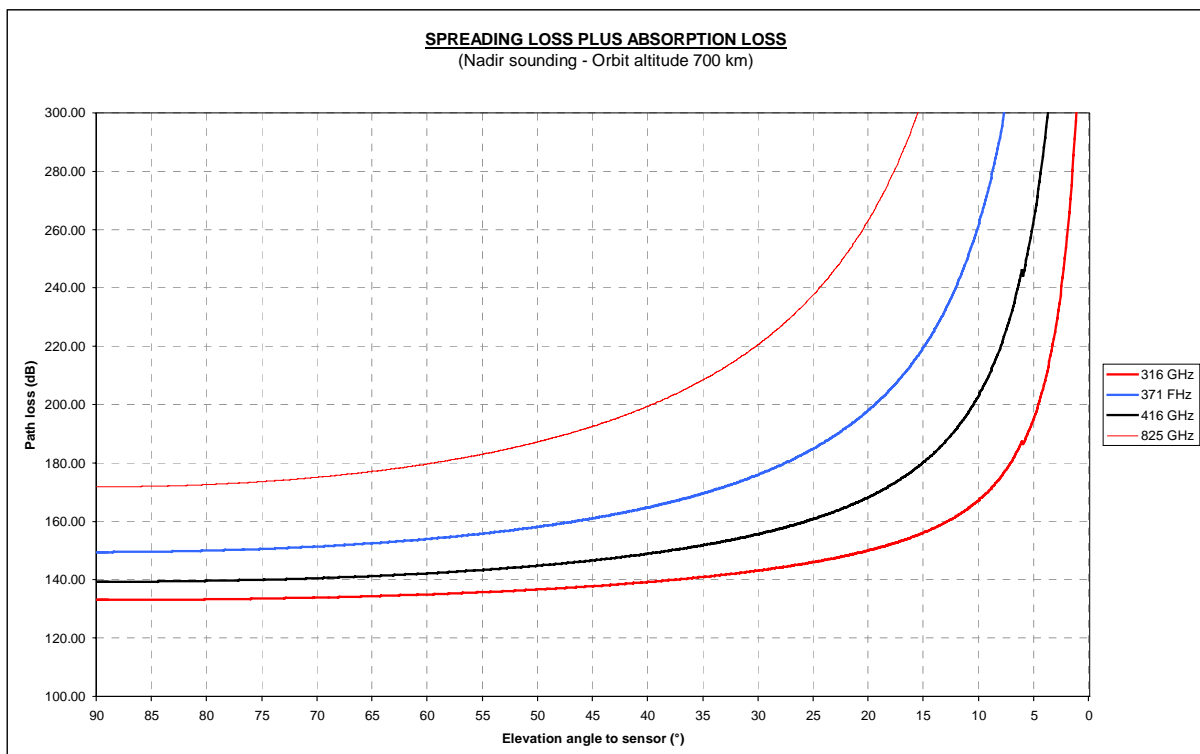
**Table 5.1.1** : Frequency bands and minimum vertical absorption

Frequency range (GHz)	Measurement	Min. vertical opacity (dB)
316-334	H <sub>2</sub> O profiling	5.15
371-389	H <sub>2</sub> O profiling.	21.6
416-434	O <sub>2</sub> profiling	11.4
546-568	H <sub>2</sub> O profiling	945
743-761	H <sub>2</sub> O profiling.	838
825-843	O <sub>2</sub> profiling	43.9
342-349	Window channel	5.3
496-506 ( ? )	Window channel	35
684-692 ( ? )	Window channel	37.6
851-853 ( ? )	Window channel	39.8

*5.1.2.2 : Path loss between the earth's surface and the sensor depending on the elevation angle*

The path loss includes the spreading loss and the absorption due to the atmosphere which increases drastically at very low elevation angles due to the geometric « lengthening factor » (re.section 4.1.2.2). Ignoring the frequencies 546 and 743 GHz where the absorption is extremely high, the *figure 5.1.2* shows the path loss at the remaining four most critical selected frequencies which may be suitable for water vapour and temperature vertical sounding. Note that the scanning of the instrument covers only the range 30°-90° elevation angles

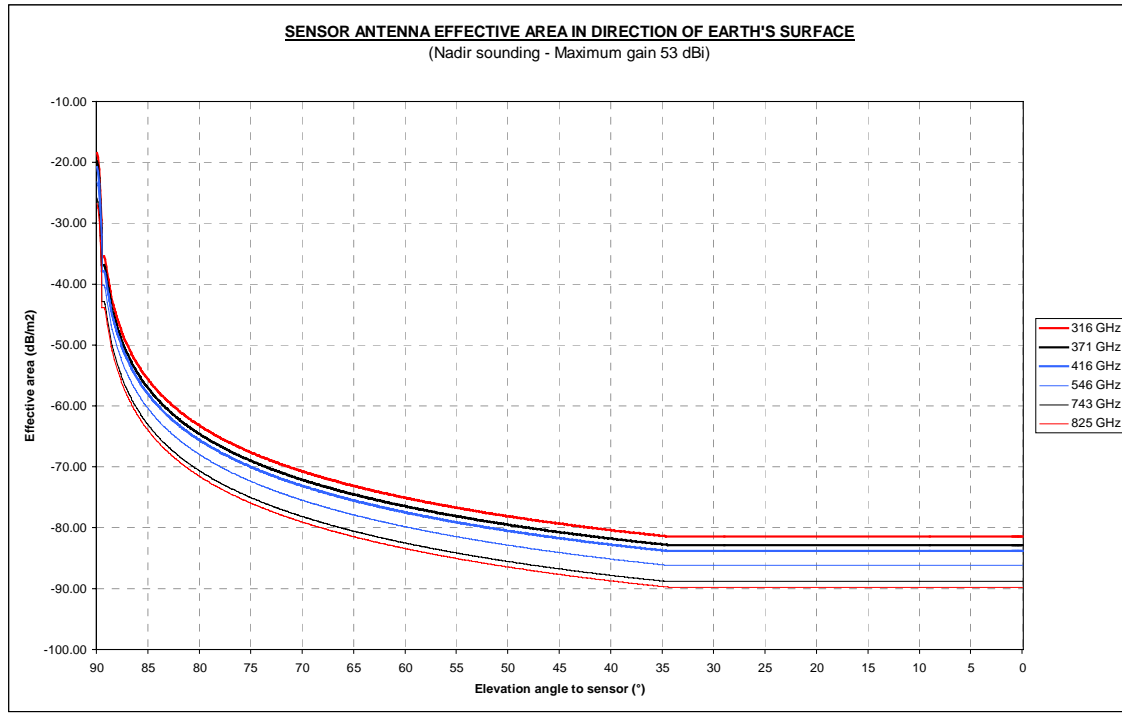
**Figure 5.1.2** : Total propagation losses between the earth's surface and the sensor



### 5.1.2.3 : Effective area of the sensor's antenna in direction of the earth's surface

The figure 5.1.3 shows the effective area of the sensor's antenna at six selected frequencies and in the worst case when the antenna is pointing in the nadir direction.

**Figure 5.1.3** : Sensor antenna effective area in direction of the earth's surface



### 5.1.2.4 : Maximum acceptable EIRP density in direction of the sensor

The maximum acceptable EIRP density in direction of the sensor is computed depending on the required radiometric performance and on the position of the interferer in the visibility circle of the sensor. The following configurations are considered :

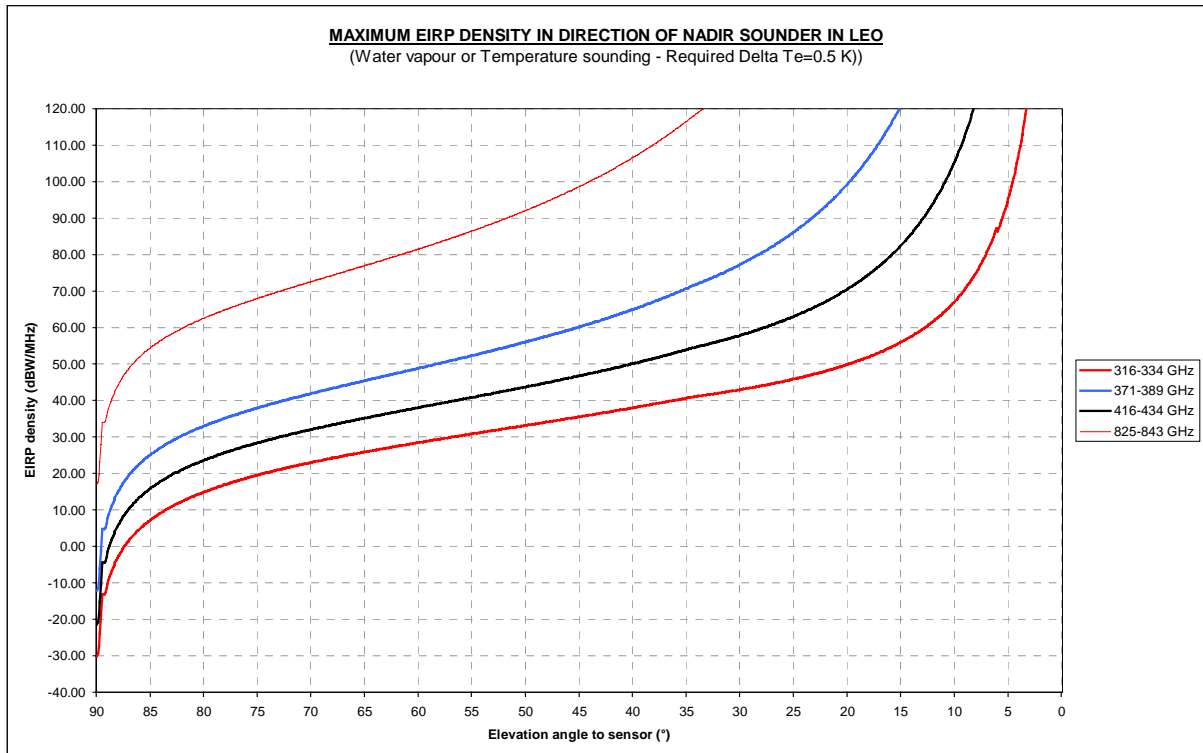
- ✕ Three values of the radiometric resolution  $\Delta T_e = 0.5 / 0.1 / 0.02 \text{ K}$  are taken into account. The corresponding contributions of the « Active terrestrial service » to the interference thresholds are respectively **-182 / -189 / -196 dBW/MHz** (re.table 3.2).

This calculation uses the total path loss and the antenna effective area determined in sections 5.1.2.2 & 5.1.2.3. It must be emphasized that «Maximum acceptable EIRP density » means that **one single terminal transmitting this EIRP density** in the receiver bandwidth of the sensor actually reaches the interference threshold of the sensor. The results are shown on *figures 5.1.4, 5.1.5 and 5.1.6*, for the three values of  $\Delta T_e$  respectively, and at six selected frequencies. A summary of the spread sheet showing the numerical results for high elevation angles is given in the *table 5.1.3*.

## 5.1.3 : Results of the analysis

The curves on the figures 5.1.4, 5.1.5 and 5.1.6 show clearly that the three lowest frequencies 316, 371 and 416 GHz, where the protection due to atmospheric absorption is the weakest, are the most vulnerable to interfering power generated by the « Active terrestrial service ». At upper frequencies 546, 743 and 825 GHz, nadir sounders are at least 30 dB less vulnerable.

Figure 5.1.4 : Maximum EIRP density for required  $\Delta T_e = 0.5$  K



The global acceptable EIRP density is the aggregate of single-entry contributions from all ground transmitters which are within the pixel of the passive sensor, and further must be apportioned among the expected population of ground transmitters that are contained in the pixel.

The single-entry EIRP density is derived from the estimated maximum number of ground transmitters which might be deployed in the pixel of the passive sensor. The maximum link density is estimated on the basis of linear absorption at ground level (re.figure 2.2). The results are summarized in the table 5.1.2. for the three optional values of the radiometric resolution.

Table 5.1.2 : Summary results of the analysis for nadir sounders in LEO

	316 GHz	371 GHz	416 GHz	546 GHz	743 GHz	825 GHz
Linear abs.(dB)	6	20	15			50
Link dens.(km-2)	2	6	4			50
<b>Maximum global EIRP density LEO (dBW/MHz)</b>						
Delta $T_e = 0.5$ K	-30	-12	-22			17
Delta $T_e = 0.1$ K	-37	-19	-29			10
Delta $T_e = 0.02$ K	-44	-26	-36			3
Pxl size	20	20	20			20
Nb.links in pxl	40	120	80			1000
Apportionment (dB)	16	21	19			30
<b>Maximum single- entry EIRP density LEO (dBW/MHz)</b>						
Delta $T_e = 0.5$ K	-46	-33	-41			-13
Delta $T_e = 0.1$ K	-53	-40	-48			-20
Delta $T_e = 0.02$ K	-60	-47	-55			-27

**A general conclusion on the sharing feasibility in the various frequency bands will be proposed after consideration of the nadir sounders in geostationary orbit. It will be seen in the section 5.2 that the results for nadir sounders in GEO are fairly similar, although slightly less critical.**



Figure 5.1.5 : Maximum acceptable EIRP density for required  $\Delta T_e = 0.1$  K

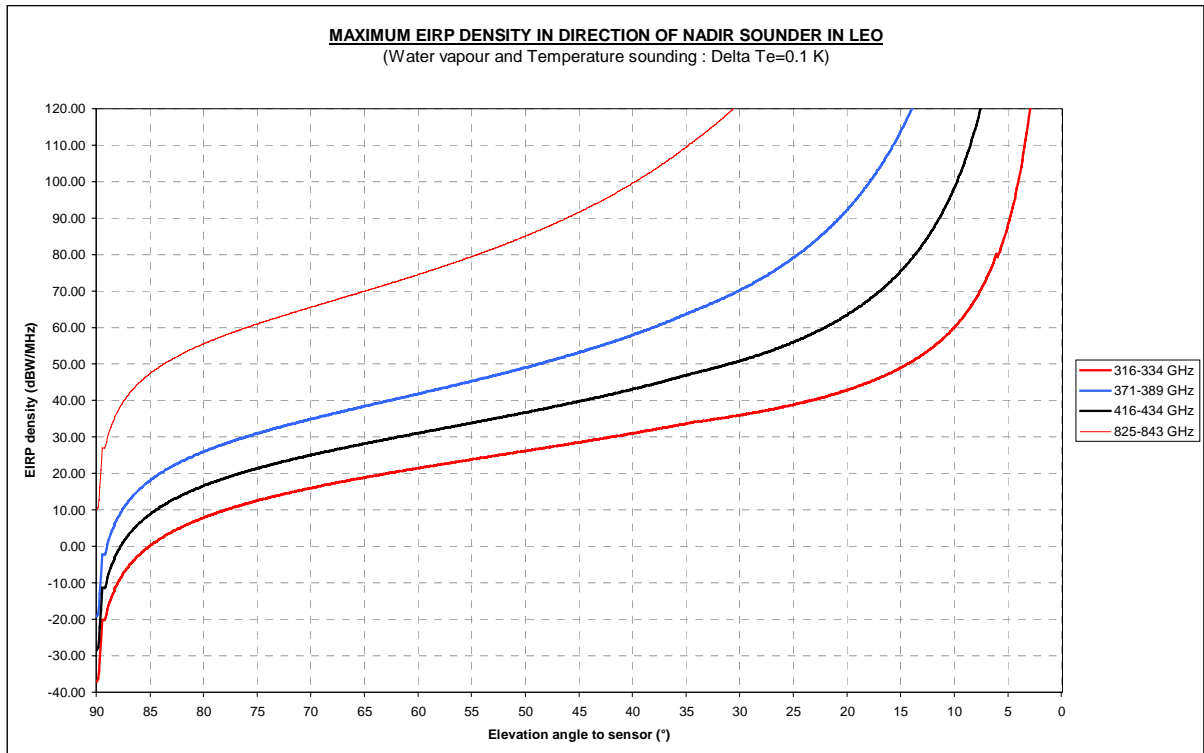
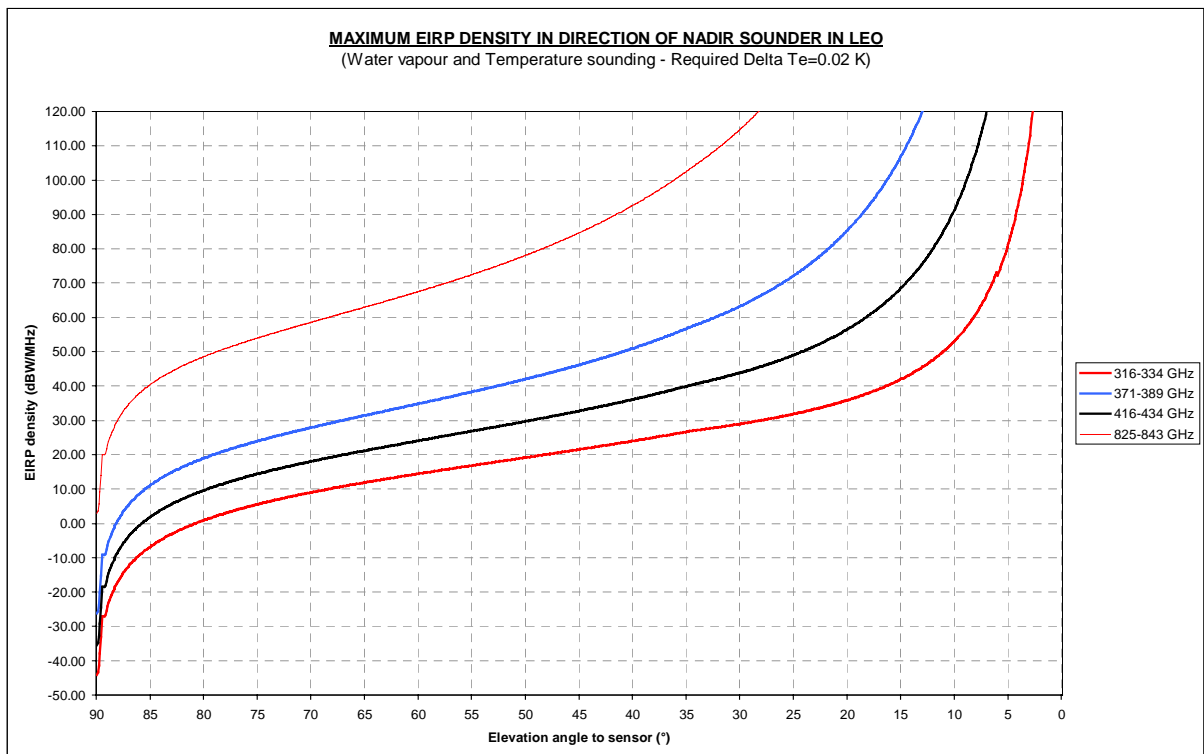


Figure 5.1.6 : Maximum acceptable EIRP density for required  $\Delta T_e = 0.02$  K





## 5.2 : Budget of potential interference to nadir sounders in GSO from the Active terrestrial service

### 5.2.1 : Geometry of interference :

The sensor's antenna is pointing in direction of the earth's surface and is scanned in the longitudinal and latitudinal directions within  $\pm 8.2^\circ$  re.the nadir direction. The scanning angle is determined in order not to exceed  $70^\circ$  incidence angle at ground level.

It should be emphasized that, in this specific configuration, the geometry of observation of the various climatic zones (defined by their latitude) is much variable in terms of distance and elevation angle, depending on their distance to the sub-satellite point. Obviously the climatic zones must be considered individually with their specific atmospheric opacities in order to identify the worst case. The *table 5.2.1* compare the specific characteristics of the three climatic zones considered, at the six frequencies selected for the study (re. Table 5.1.1).

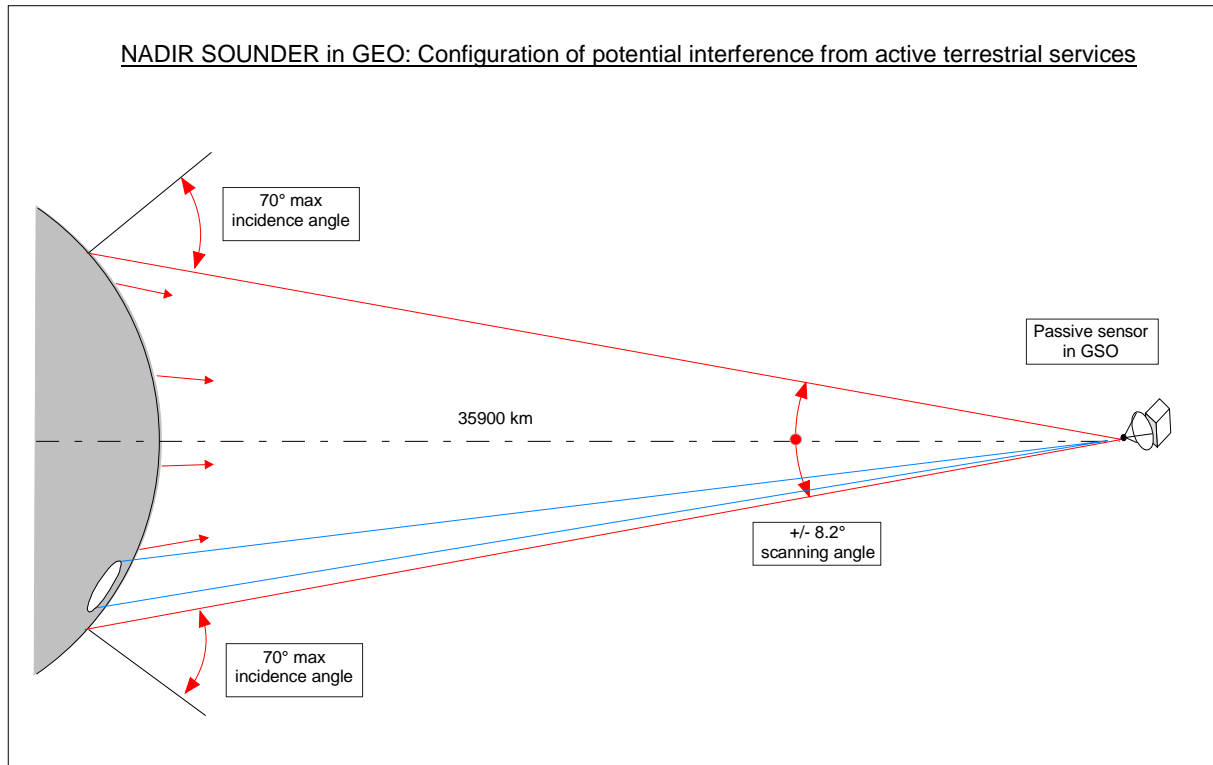
Table 5.2.1 : Specific features of climatic zones as seen from the nadir sounder in GSO

	Sub-Arctic Winter	Mid-Latitude Winter	Tropical
	<b>Vertical opacity (dB)</b>		
316 GHz	5.15	9.93	47.70
371 GHz	21.60	40.80	182.00
416 GHz	11.40	21.10	95.90
546 GHz	945.00	1770.00	7070.00
743 GHz	838.00	1590.00	6510.00
825 GHz	43.90	84.80	407.00
	<b>Geometric features</b>		
Latitude ( $^\circ$ )	61.00	45.00	0.00
Shortest distance (km)	39600.00	38100.00	35900.00
Spreading loss incr.(dB)	0.85	0.52	0.00
Elevation angle ( $^\circ$ )	20.00	38.00	90.00
Lengthening factor	2.92	1.62	1.00
	<b>Slant opacity integrating the lengthening factor (dB)</b>		
316 GHz	15.06	16.13	47.70
371 GHz	63.15	66.27	182.00
416 GHz	33.33	34.27	95.90
546 GHz	2763.00	2874.96	7070.00
743 GHz	2450.15	2582.59	6510.00
825 GHz	128.36	137.74	407.00

Comparing the various parameters shown in this table, it is clear that frequencies 546 and 743 GHz do not need to be further considered in the study, due to the extremely high atmospheric absorption. It is noted that Sub-Arctic winter and Mid-Latitude winter zones are almost equivalent at all frequencies, particularly at the three lowest ones (see the slant opacity and the spreading loss difference). This difference is further reduced by the increased surface of the sensor's antenna foot print at the lowest elevation angle. It can be concluded that the worst case is the observation of medium to high latitude areas. The analysis is performed for the highest latitudes reached by the sensor, which may need more severe constraints to be placed on the terrestrial services, due to the low elevation of the interfering path, and is considered valid also for the mid-latitude regions.

Similarly to the LEO case, the sensor can receive interference essentially via its main lobe, from ground transmitters which are located within the « pixel » of the passive sensor, assumed to be limited by the half-power beamwidth of the antenna. The sensor's antenna is assumed to be pointed at  $25^\circ$  elevation angle. The configuration is illustrated on the *figure 5.2.1*.

Figure 5.2.1 : Geometry of potential interference from active terrestrial services



### 5.2.2 : Maximum acceptable interfering power density

The calculations implemented in the section 5.1 for nadir sounders in LEO are re-iterated, using the geometric parameters and the sensor's antenna gain that are specific to the GSO configuration.

The intermediate results, spreading loss + absorption loss and antenna effective area that are necessary to establish the potential interference budget, are shown on *figure 5.2.2* and *figure 5.2.3* respectively, at the four frequencies retained for analysis.

The maximum acceptable EIRP densities in direction of the sensor are then computed. The results are shown on the *figures 5.2.4, 5.2.5 and 5.2.6*. Numerical results are summarized in *the table 5.2.2*.

Figure 5.2.2 : Total propagation losses between the earth's surface and the sensor

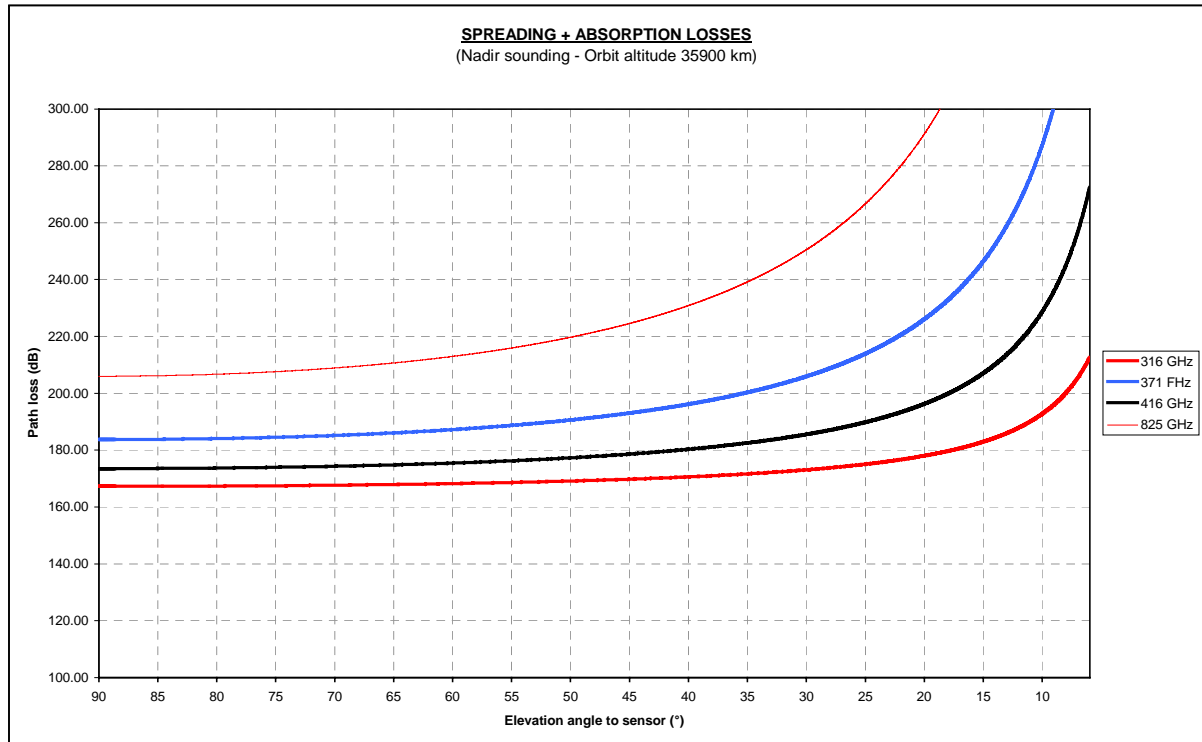


Figure 5.2.3 : Sensor antenna effective area in direction of the earth's surface

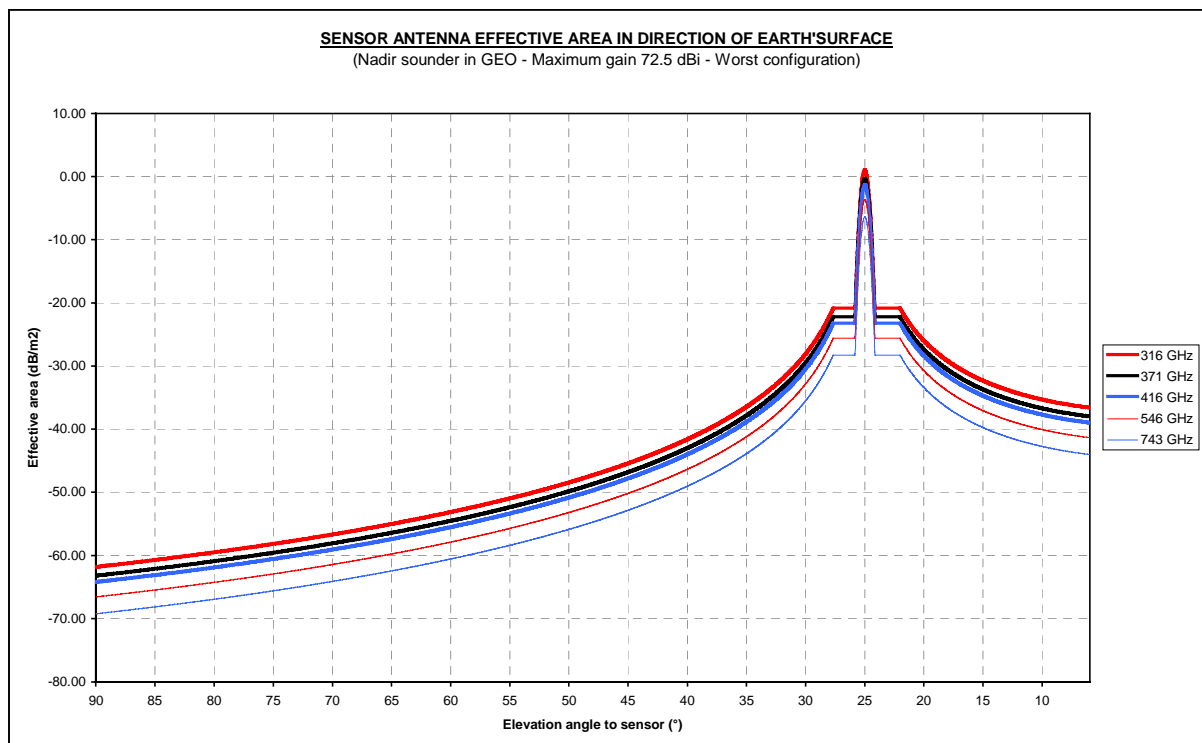


Figure 5.2.4 : Maximum EIRP density for required  $\Delta T_e = 0.5$  K

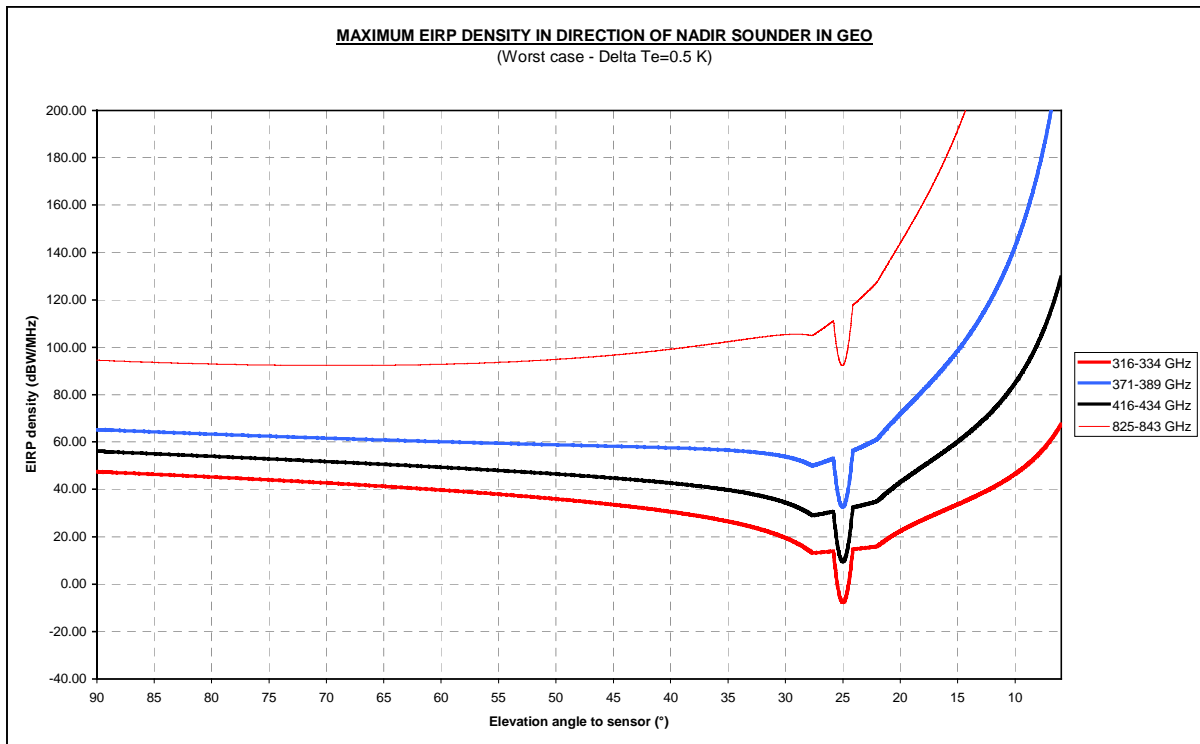


Figure 5.2.5 : Maximum acceptable EIRP density for required  $\Delta T_e = 0.1$  K

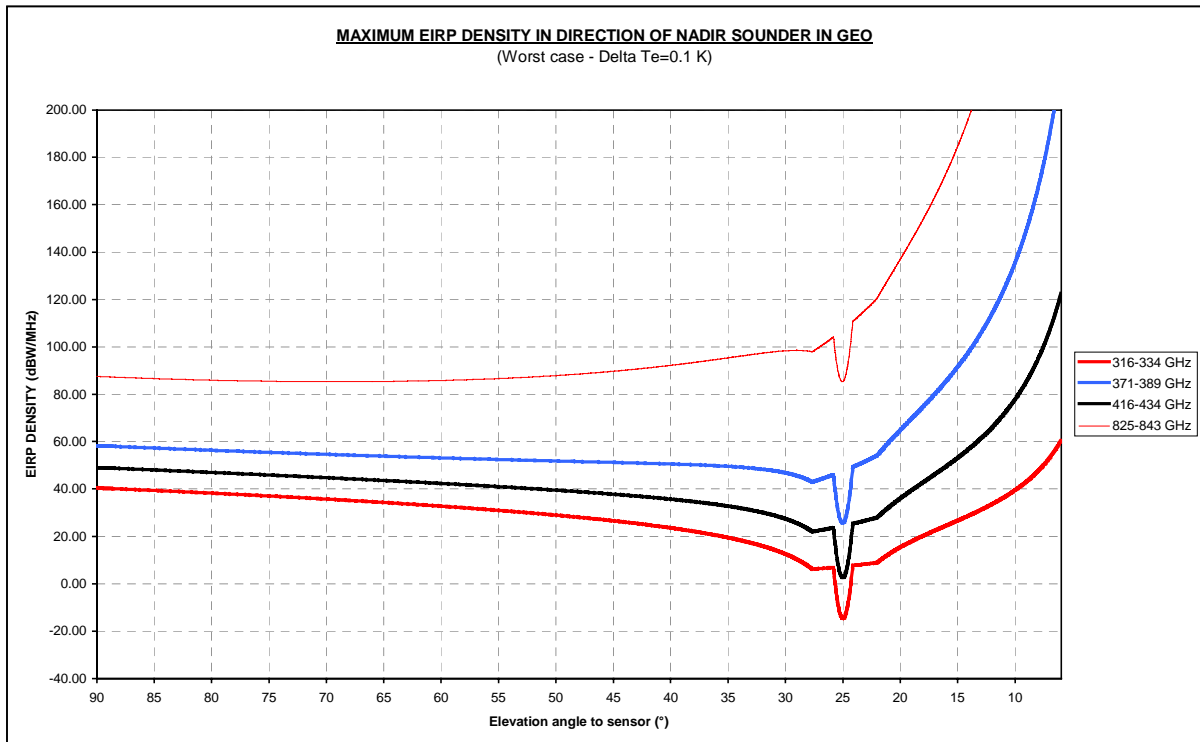
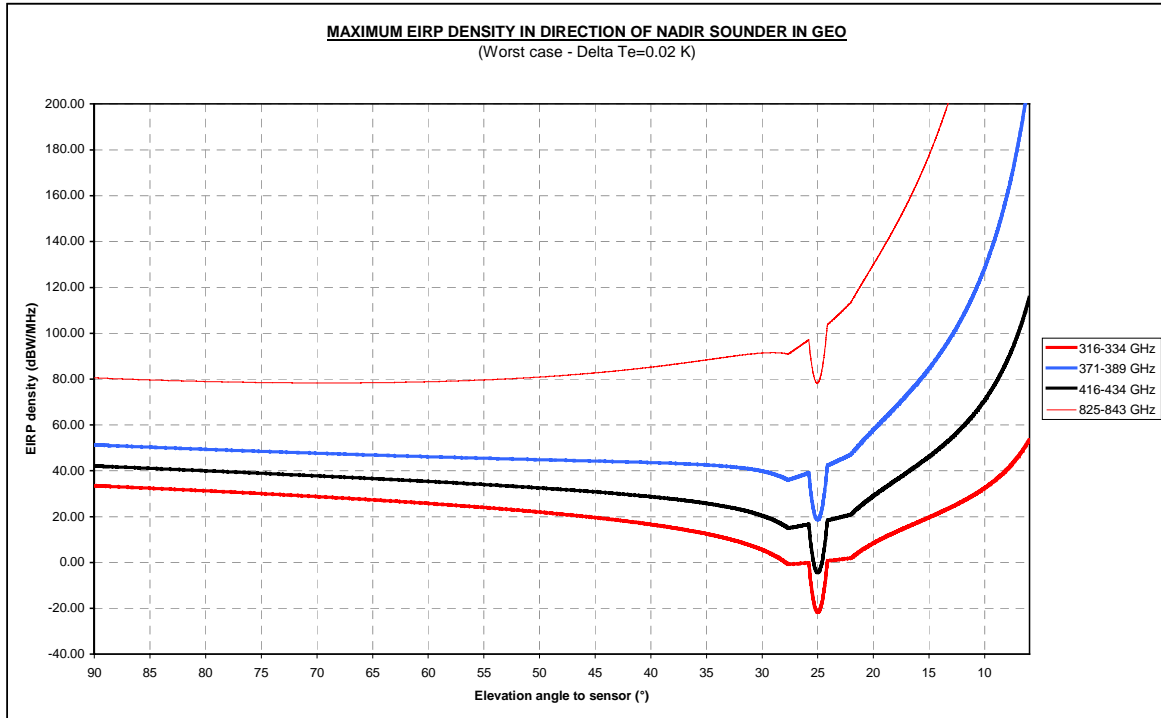




Figure 5.2.6 : Maximum required EIRP density for required  $\Delta T_e = 0.02$  K



### 5.2.3 :Results of the analysis

As explained in section 5.1.3, the global EIRP density is apportioned among the population of terrestrial transmitters which are within the sensor’s antenna foot-print. The results and the parameters used are summarized in the *table 5.2.2*, which also repeats the results obtained for the nadir sounder in LEO.

Table 5.2.2 : Summary results of the analysis for nadir sounders in GSO and LEO

	316 GHz	371 GHz	416 GHz	546 GHz	743 GHz	825 GHz
Linear abs.(dB)	6	20	15			50
Link dens.(km-2)	2	6	4			50
<b>Global EIRP density GSO (dBW/MHz)</b>						
Delta Te = 0.5 K	-8	33	10			92
Delta Te = 0.1 K	-15	26	3			85
Delta Te = 0.02 K	-22	19	-4			78
Pxl size (km2)	1160	1160	1160			1160
Nb.links in pxl	2320	6960	4640			58000
Apportionment (dB)	34	38	37			48
<b>Single-entry EIRP density GSO (dBW/MHz)</b>						
Delta Te = 0.5 K	-41	-6	-27			45
Delta Te = 0.1 K	-48	-13	-34			38
Delta Te = 0.02 K	-55	-20	-41			31
<b>Maximum global EIRP density LEO (dBW/MHz)</b>						
Delta Te = 0.5 K	-30	-12	-22			17
Delta Te = 0.1 K	-37	-19	-29			10
Delta Te = 0.02 K	-44	-26	-36			3
Pxl size	20	20	20			20
Nb.links in pxl	40	120	80			1000
Apportionment (dB)	16	21	19			30
<b>Maximum single- entry EIRP density LEO (dBW/MHz)</b>						
Delta Te = 0.5 K	-46	-33	-41			-13
Delta Te = 0.1 K	-53	-40	-48			-20
Delta Te = 0.02 K	-60	-47	-55			-27



## 5.3 : Budget of potential interference from the Inter-Satellite Service

### 5.3.1 : Geometry of interference :

Nadir sounders include a hot calibration system and a cold space calibration system which are activated at each earth scanning sequence of the instrument. They provide calibration parameters that are essential for the processing of the geophysical data acquired by the instrument. The cold space system requires an antenna pointing towards a cold region of the sky, similarly to a limb sounder. This can use the main receiving chain of the sensor taking advantage of the mechanical scanning of the instrument, or can require a specific antenna.

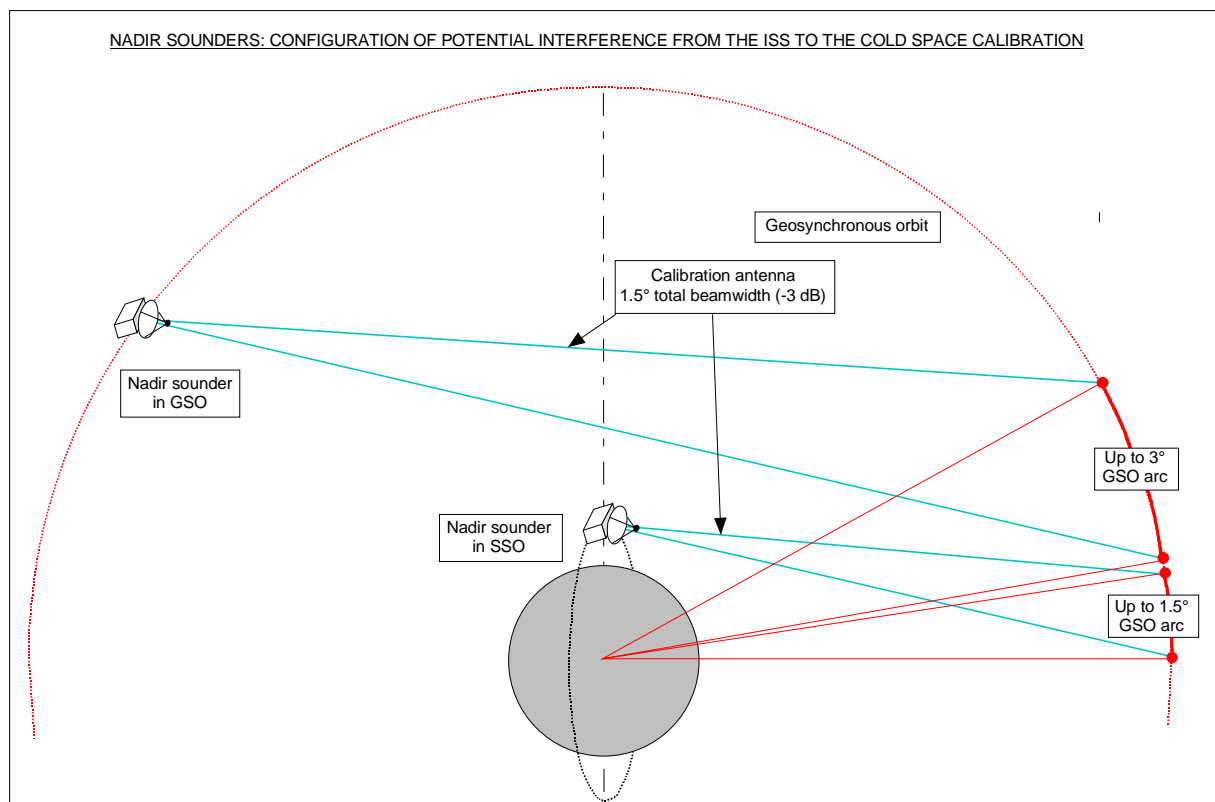
This latter option is selected for the study, because the utilization of a specific antenna with isotropic gain smaller than the main antenna gain, renders the calibration system less vulnerable to interference produced by links of the ISS, although its wider beam can intercept more than one satellite of the ISS.

Past studies on passive sensors in the 60/118/183 GHz frequency range concluded that co-frequency sharing with links of the **ISS in non-geostationary orbits is not feasible** due to the vulnerability of the cold space calibration of the passive sensors:

- As a consequence, the present study considers **exclusively co-frequency sharing with links of the ISS between satellites in geostationary orbit**.

It is noted that the minimum longitudinal separation between satellites of GSO system of the ISS on their common orbit is  $1^\circ$  (long range link), and that several orbits of various inclination angles are envisaged. The configuration is illustrated in the *figure5.3.1*.

Figure 5.3.1 : Geometry of potential interference from the ISS



### 5.3.2 : Maximum acceptable single-entry power flux density in the environment of the sensor :

Links between satellites of an ISS system can aim at almost any position of the geosynchronous orbits that can be used by the ISS. The interfering power received by the passive sensor in low earth orbit (LEO) depends on the distance between each satellite of the ISS and the passive sensor and on the EIRP in direction of the LEO. These are varying parameters which cannot be easily predicted and therefore cannot be converted into a unique sharing criteria applicable to all links of the ISS.

The sharing criteria already adopted in similar sharing situations around 60 GHz, 118 GHz and 183 GHz is the power flux density (PFD) at the level of the passive sensor's antenna, which depends only on the interference threshold of the sensor and on the effective area of the cold space calibration antenna.

- ✘ Three optional values of the radiometric resolution  $\Delta T_e = 0.5 / 0.1 / 0.02 \text{ K}$  are considered. The corresponding thresholds applicable to the Inter-Satellite Service are respectively  $-182 / -189 / -196 \text{ dBW/MHz}$ .

It is assumed that the isotropic gain of the cold space calibration antenna is 35 dBi for both LEO and GSO nadir sounders. From a LEO orbit, the calibration antenna can intercept an  $1.5^\circ$  arc (half-power beamwidth) of the geosynchronous orbit twice per orbit period. From a GSO orbit the calibration antenna can intercept almost permanently about twice this angle. In both cases it is assumed that two or more satellites of the ISS can simultaneously be in the main lobe of the calibration antenna. 3 dB / 5 dB margins for multiple entries are therefore adopted for LEO and GSO respectively, to derive the single-entry pfd limits. The results are summarized in the *table 5.3.2*.

Table 5.3.2 : Single-entry pfd limit at the level of nadir sounders in LEO and in GSO

<b>NADIR SOUNDERS IN LEO AND IN GSO</b>							
<b>RADIOMETER</b>							
<b>Ant.gain (dB)</b>	35.0						
<b>Rad.resolution (K)</b>	0.500		0.100	0.020			
<b>Rad.bandwidth (MHz)</b>	1		1	1			
<b>Rad.threshold (dBW/MHz)</b>	-171.61		-178.60	-185.59			
<b>Int.thresh.(dBW/MHz)</b>	-178.61		-185.60	-192.59			
<b>Apportioned to the ISS</b>	-181.61		-188.60	-195.59			
			<b>Global p.f.d.limit (dBW/MHz/m2)</b>				
<b>Freq.(GHz)</b>	<b>Lambda (m)</b>	<b>Ef.ar.(dB/m2)</b>	<b>0.5 K</b>	<b>0.1 K</b>	<b>0.02 K</b>		
316	9.49E-04	-3.64E+01	-145.17	-152.16	-159.15		
371	8.09E-04	-3.78E+01	-143.77	-150.76	-157.75		
416	7.21E-04	-3.88E+01	-142.78	-149.77	-156.76		
546	5.49E-04	-4.12E+01	-140.42	-147.41	-154.40		
743	4.04E-04	-4.39E+01	-137.74	-144.73	-151.72		
825	3.64E-04	-4.48E+01	-136.83	-143.82	-150.81		
			<b>Single-entry p.f.d.limit (dBW/MHz/m2)</b>				
			<b>NADIR SOUNDER IN LEO</b>			<b>NADIR SOUNDER IN GSO</b>	
<b>Freq.(GHz)</b>	<b>0.5 K</b>	<b>0.1 K</b>	<b>0.02 K</b>	<b>0.5 K</b>	<b>0.1 K</b>	<b>0.02 K</b>	
316	-148.17	-155.16	-162.15	-150.17	-157.16	-164.15	
371	-146.77	-153.76	-160.75	-148.77	-155.76	-162.75	
416	-145.78	-152.77	-159.76	-147.78	-154.77	-161.76	
546	-143.42	-150.41	-157.40	-145.42	-152.41	-159.40	
743	-140.74	-147.73	-154.72	-142.74	-149.73	-156.72	
825	-139.83	-146.82	-153.81	-141.83	-148.82	-155.81	

### 5.3.3 : Preliminary conclusion :

Passive sensors in LEO and inter-satellite links of GSO satellite systems can share the same frequency bands in the 275 to 1000 GHz spectral region provided that the single-entry power flux-density at all altitudes from 0 to 1000 km above the Earth's surface (case of the nadir sounders in LEO) and in the vicinity of all geostationary orbital positions occupied by passive sensors (case of nadir sounders in GSO), produced by a station in the inter-satellite service, for all conditions and for all methods of modulation, shall not exceed [ refer to the table 5.3.2 ] for all angles of arrival.

It is anticipated that the condition concerning the nadir sounders in GSO will not be easy to implement.

## 6.0 : GENERAL SUMMARY

Considering three optional performance levels for limb sounders and for nadir sounders, the study has established a set of conditions, EIRP densities for co-frequency sharing with terrestrial services and spectral PFD's for co-frequency sharing with the ISS, under which co-frequency sharing would be feasible. The specific conclusions for each scenario considered are summarized in the tables/figures that follows :

**Table 6.1** : Limb sounders : single-entry EIRP density limits applicable to ground transmitters

<b>Frequency range (GHz) :</b>	<b>275-375</b>	<b>475-750</b>	<b>775-1000</b>
<b>Single entry EIRP density limit (dBW/MHz)</b>			
Range of Elevation (°):	3 to 90	20 to 90	20 to 90
For $\Delta T = 0.1$ K :	-20	6	13
For $\Delta T = 0.01$ K :	-30	-4	3
For $\Delta T = 0.001$ K :	-40	-14	-7

**Figure 6.1** : Limb sounders : Maximum single-entry spectral PFD at the level of the sensor

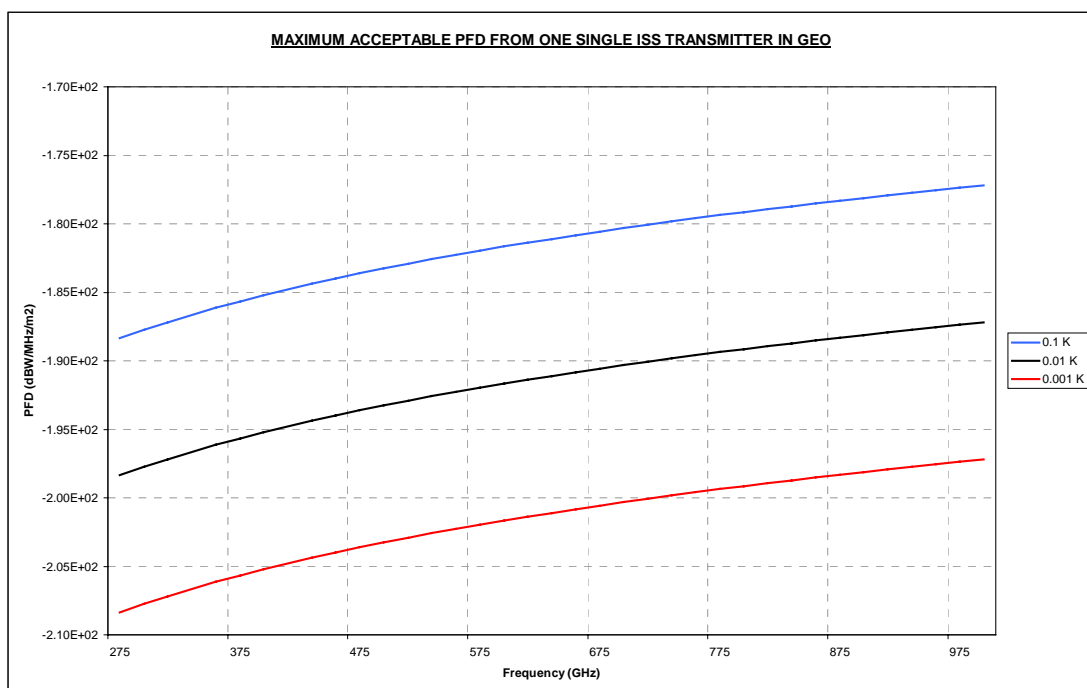


Table 6.2 : Nadir sounders in GSO and LEO : Maximum EIRP density from terrestrial service

	316 GHz	371 GHz	416 GHz	546 GHz	743 GHz	825 GHz
Linear abs.(dB)	6	20	15			50
Link dens.(km-2)	2	6	4			50
<b>Global EIRP density GSO (dBW/MHz)</b>						
Delta Te = 0.5 K	-8	33	10			92
Delta Te = 0.1 K	-15	26	3			85
Delta Te = 0.02 K	-22	19	-4			78
Pxl size (km2)	1160	1160	1160			1160
Nb.links in pxl	2320	6960	4640			58000
Apportionment (dB)	34	38	37			48
<b>Single-entry EIRP density GSO (dBW/MHz)</b>						
Delta Te = 0.5 K	-41	-6	-27			45
Delta Te = 0.1 K	-48	-13	-34			38
Delta Te = 0.02 K	-55	-20	-41			31
<b>Maximum global EIRP density LEO (dBW/MHz)</b>						
Delta Te = 0.5 K	-30	-12	-22			17
Delta Te = 0.1 K	-37	-19	-29			10
Delta Te = 0.02 K	-44	-26	-36			3
Pxl size	20	20	20			20
Nb.links in pxl	40	120	80			1000
Apportionment (dB)	16	21	19			30
<b>Maximum single- entry EIRP density LEO (dBW/MHz)</b>						
Delta Te = 0.5 K	-46	-33	-41			-13
Delta Te = 0.1 K	-53	-40	-48			-20
Delta Te = 0.02 K	-60	-47	-55			-27

Table 6.3 : Nadir sounders in LEO and in GSO : Single-entry spectral PFD from the ISS

<b>NADIR SOUNDERS IN LEO AND IN GSO</b>							
<b>RADIOMETER</b>							
Ant.gain (dB)	35.0						
Rad.resolution (K)	0.500	0.100	0.020				
Rad.bandwidth (MHz)	1	1	1				
Rad.threshold (dBW/MHz)	-171.61	-178.60	-185.59				
Int.thresh.(dBW/MHz)	-178.61	-185.60	-192.59				
Apportioned to the ISS	-181.61	-188.60	-195.59				
			<b>Global p.f.d.limit (dBW/MHz/m2)</b>				
Freq.(GHz)	Lambda (m)	Ef.ar.(dB/m2)	0.5 K	0.1 K	0.02 K		
316	9.49E-04	-3.64E+01	-145.17	-152.16	-159.15		
371	8.09E-04	-3.78E+01	-143.77	-150.76	-157.75		
416	7.21E-04	-3.88E+01	-142.78	-149.77	-156.76		
546	5.49E-04	-4.12E+01	-140.42	-147.41	-154.40		
743	4.04E-04	-4.39E+01	-137.74	-144.73	-151.72		
825	3.64E-04	-4.48E+01	-136.83	-143.82	-150.81		
			<b>Single-entry p.f.d.limit (dBW/MHz/m2)</b>				
			<b>NADIR SOUNDER IN LEO</b>			<b>NADIR SOUNDER IN GSO</b>	
Freq.(GHz)	0.5 K	0.1 K	0.02 K	0.5 K	0.1 K	0.02 K	
316	-148.17	-155.16	-162.15	-150.17	-157.16	-164.15	
371	-146.77	-153.76	-160.75	-148.77	-155.76	-162.75	
416	-145.78	-152.77	-159.76	-147.78	-154.77	-161.76	
546	-143.42	-150.41	-157.40	-145.42	-152.41	-159.40	
743	-140.74	-147.73	-154.72	-142.74	-149.73	-156.72	
825	-139.83	-146.82	-153.81	-141.83	-148.82	-155.81	

- ⊠ Clearly limb sounders, due to their high antenna gain and due to their specific configuration, are significantly more vulnerable to interference generated by systems of the ISS in GSO than the nadir sounders. Acceptable interfering levels might be too low to be practical for the ISS, making co-frequency sharing between the ISS and the limb sounders impossible.
- ⊠ Sharing between nadir sounders in GSO and systems of the ISS requires that positions of EESS satellites carrying nadir sounders are clearly and definitely identified in advance. This may be difficult to implement, considering in particular that meteorological satellites in GSO may require to be temporarily shifted on the geostationary orbit to implement particular scientific experiments, or to fill a gap in the global coverage.
- ⊠ Nadir sounders are significantly more vulnerable to interference produced by active terrestrial services than limb sounders. Maximum acceptable EIRP densities are very low at the lower frequencies. However, in the ignorance of the nature and of the operational/technical characteristics of terrestrial service that might use this spectral region, it would be very premature to draw any conclusion on the practicability of co-frequency sharing.
- ⊠ The Article S5 of the Radio Regulations published by the ITU contains the table of frequency allocations to the various services which are using the spectrum. To make it reflect the evolution of requirements, this table of allocations needs reviewing and updating on a regular basis. This is done every two or three years in average, in the framework of World Radio Conferences (WRC) convened by the ITU. The last revision adopted by the WRC-2000 (May/June 2000, Istanbul) covered the spectrum up to 275 GHz, but there is for the time being no allocation above 275 GHz.

The extension for frequencies above 275 GHz and up to 1000 GHz requires that study programmes are initiated and conducted on a co-ordinated basis under the auspices of the ITU, with the following general objectives aiming at the elaboration of a table of allocations :

- To determine the needs of the various services in terms of spectrum requirements ;
- To determine their technical characteristics ;
- To evaluate the feasibility and constraints of co-frequency sharing between different services.

The services of scientific nature, such as the Earth Exploration Satellite Service, are certainly the most advanced in their plans of spectrum requirements and utilization above 275 GHz. The present study concentrates on the passive sensors of the EESS. However, because the scientific expertise in the utilization of this spectral region is still at an early stage, and because the nature and the characteristics of the other (active) services which might share the same frequency bands are unknown, it is recognized that conclusions which are proposed are preliminary and should be considered as a basis for further work and, as such, should serve as the trigger for the definition and adoption of co-ordinated study programme(s) by the ITU in the perspective of a future WRC. On the scientific side, it will be necessary to consolidate the requirements in particular :

- Confirm or amend the spectrum requirements and eliminate any possible redundancy ;
- Confirm the measurement objectives in terms of radiometric and spatial resolutions, and in terms of operational configurations ;
- Contribute to new sharing studies whenever objectives and characteristics of « active » services will be clarified.